

Dark energy with a gradient coupling to the dark matter fluid: cosmological dynamics and structure formation

Jibitesh Dutta,^{a,b} Wompherdeiki Khylllep,^{c,d} Nicola Tamanini^e

^aMathematics Division, Department of Basic Sciences and Social Sciences, North Eastern Hill University, NEHU Campus, Shillong, Meghalaya 793022, India

^bInter University Centre for Astronomy and Astrophysics, Pune 411 007, India

^cDepartment of Mathematics, North Eastern Hill University, NEHU Campus, Shillong, Meghalaya 793022, India

^dDepartment of Mathematics, St. Anthony's College, Shillong, Meghalaya 793001, India

^eInstitut de Physique Théorique, CEA-Saclay, CNRS UMR 3681, Université Paris-Saclay, F-91191 Gif-sur-Yvette, France

E-mail: jdutta29@gmail.com, jdutta@associates.iucaa.in,
sjwomkhylllep@gmail.com, nicola.tamanini@cea.fr

Abstract. We consider scalar field models of dark energy interacting with dark matter through a coupling proportional to the contraction of the four-derivative of the scalar field with the four-velocity of the dark matter fluid. The coupling is realized at the Lagrangian level employing the formalism of Scalar-Fluid theories, which use a consistent Lagrangian approach for relativistic fluid to describe dark matter. This framework produces fully covariant field equations, from which we can derive unequivocal cosmological equations at both background and linear perturbations levels. The background evolution is analyzed in detail applying dynamical systems techniques, which allow us to find the complete asymptotic behavior of the universe given any set of model parameters and initial conditions. Furthermore we study linear cosmological perturbations investigating the growth of cosmic structures within the quasi-static approximation. We find that these interacting dark energy models give rise to interesting phenomenological dynamics, including late-time transitions from dark matter to dark energy domination, matter and accelerated scaling solutions and dynamical crossing of the phantom barrier. Moreover we obtain possible deviations from standard Λ CDM behavior at the linear perturbations level, which have an impact on the dynamics of structure formation and might provide characteristic observational signatures.

Contents

1	Introduction	1
2	Scalar-Fluid theories with a derivative coupling	3
2.1	The Scalar-Fluid action	3
2.2	Background cosmological equations	4
3	Background cosmological dynamics	5
3.1	Formation of the autonomous system	5
3.2	Model I	6
3.2.1	$(0, 0)$ model	7
3.2.2	$(1, 0)$ model	9
3.2.3	$(1, \frac{1}{2})$ model	12
3.3	Model II	14
3.3.1	$\beta = 0$ case	16
3.3.2	$\beta = 1$ case	18
4	Cosmological perturbation and structure formation	18
4.1	Linear perturbations and quasi-static approximation	18
4.2	Model I	20
4.2.1	$(0, 0)$ model	20
4.2.2	$(0, \frac{1}{2})$ model	21
4.2.3	$(1, 0)$ model	22
4.2.4	$(1, \frac{1}{2})$ model	23
4.3	Model II	23
5	Conclusion	25
A	Appendix: Center Manifold Theory (CMT)	26
A.1	General framework	26
A.2	Applications of CMT	27

1 Introduction

Although various astrophysical observations have by now confirmed the present accelerated expansion of our universe [1–5], a search for the exact nature of the phenomenon driving this acceleration is still under way. In order to find a theoretical explanation, two main approaches are usually considered: modifying the gravitational part of the Einstein equations [6–8] or introducing the concept of dark energy (DE) as a new mysterious cosmological component. The time-independent cosmological constant Λ is known to be the simplest DE candidate proposed so far, and it appears to be consistent with the current observations. Λ has however its own theoretical problems, specifically the so called cosmological constant problem and the cosmic coincidence problem [9–11]. In order to overcome these issues, another promising explanation for DE that has been proposed is a dynamical scalar field with a self-interacting potential which can mimic the cosmological constant behaviour at late times (see [12, 13] for

reviews). Scalar field models can moreover be well motivated by the low energy limit of well known high energy theories, for example string theory.

Once DE is allowed to be characterised by a dynamical field, it is natural to consider possible interactions with other cosmological components. An interaction between DE and ordinary matter is severely constrained by solar system experimental tests probing the magnitude of a possible fifth force [14, 15]. Nevertheless a coupling between DE and dark matter (DM) cannot be excluded by Solar System experiments and cosmological observations still allow such possibility (see e.g. [16–18]). The presence of an interaction in the dark sector is an interesting hypothesis in modern cosmology, which could have an effect on both background and perturbation dynamics [19, 20]. One of the main features of interacting DE is the existence of late time accelerated scaling attractors, which in principle can alleviate the coincidence problem [21–23]. Furthermore current observations [4, 5] mildly suggest that the effective equation of state (EoS) parameter of DE might be smaller than that of a cosmological constant, i.e. smaller than -1 . This phenomenon cannot be achieved in uncoupled canonical models with a single scalar field. A possible solution is provided by a phantom scalar field, which however suffers from classical and quantum instabilities [24, 25]. Interestingly, the crossing of the phantom divide line (i.e. the crossing of the value -1 for the EoS parameter) can also be achieved through an interaction in the dark sector, without resorting to a phantom scalar field. Some current observational datasets provide moreover some indications of a non-vanishing late time interaction [17, 26, 27], and future experiments will be able to better constrain such hypothesis [28–30].

A coupling between DE and DM could thus be used to alleviate the cosmic coincidence problem and to explain a possible excursion in the phantom regime. The problem then arises on how to define this interaction from a theoretical perspective. Due to the unknown fundamental nature of both DE and DM, any coupling proposed in the literature can only be defined phenomenologically at the level of the field equations (see e.g. [31–33]). This has created some problems whenever extensions of these models from the background dynamics to the perturbation level or full covariant level were considered [34–36], and it has moreover limited the theoretical framework describing a possible dark interaction [37]. In order to overcome these issues, a new framework of coupled DE models, generally known as Scalar-Fluid theories, was introduced in [38, 39]. In this class of theories a consistent variational approach is employed by modelling DM as a dynamical fluid using Brown’s Lagrangian formulation of relativistic fluids [40]. This allows for a well-defined, though still phenomenological, Lagrangian, able to provide fully covariant equations of motion, and thus unequivocal cosmological dynamics at both background and perturbation levels. Scalar-Fluid theories include and extend most of the previously considered interactions between scalar field DE and DM. Within their framework the scalar field’s and the fluid’s degrees of freedom can not only be coupled algebraically [38], but interacting terms between the scalar field gradient (its derivative) and the fluid’s four-velocity can be created at the Lagrangian level [39]. For some applications of Scalar-Fluid theories we refer the reader to [41–45].

In the present work, we investigate the cosmological dynamics of Scalar-Fluid DE models with the gradient (derivative) coupling introduced in [39]. We consider an arbitrary self-interacting scalar field potential and make use of dynamical system methods to characterise the background cosmic evolution in detail. Dynamical system techniques constitute a powerful tool to determine the asymptotic behavior of any cosmological model. The objective is to relate the critical points of the phase space with important cosmological periods, for example inflation, matter dominated and accelerated DE dominated eras. A similar analysis has

already been performed in [39], where however only exponential potentials were considered for the scalar field. Apart from a mathematical point of view, the generalization to arbitrary scalar field potentials, is also well motivated by the low-energy limit of more fundamental high-energy theories, as well as by comparison with different phenomenological models of DE [12, 13]. In order to analyze the cosmological dynamics for arbitrary potentials, we rely on the method developed in [46] for the quintessence field, and subsequently applied in the context of k -essence [47], braneworld theories [33, 48–50], tachyon fields [51–53], quintom fields [54] and loop quantum gravity [55]. We also discuss the stability of non-hyperbolic critical points (critical points whose Jacobian matrix present eigenvalues of vanishing real part), for which standard linear stability theory fails to determine their properties. Non-hyperbolic critical points arise in the background dynamics of different DE models and might contain important information and interesting dynamical features regarding the late time universe. To determine their stability, we either use some advanced mathematical tool such as center manifold theory [46, 56–59] or numerical computational techniques such as the analysis of perturbed trajectories near the critical point [33, 47].

Furthermore, in order to check the viability of these coupling models during the formation of large scale structures, we investigate them at the linear cosmological perturbation level. Cosmological perturbations for Scalar-Fluid theories have been first investigated in [41, 42]. In the quasi-static approximation, we used to describe the structure dynamics deep inside the horizon, new interesting modifications to the equations describing the growth of structures appear, with properties which cannot easily be obtained in other models of DE or even modified gravity. In the present paper we study the dynamics of scalar perturbations during eras of effective matter domination, where the scalar field might imprint particular features during the growth of structure, while not affecting the evolution at the background level. This analysis can be useful to identify specific signatures of Scalar-Fluid theories to look for by cosmological observations.

The organization of this paper is as follows. In Sec. 2, we briefly review the theoretical framework of Scalar-Fluid theories introduced in [39], presenting the basic cosmological equations. In Sec. 3 we explore the dynamics at the background cosmological level, starting by deriving an autonomous system of differential equations in a spatially flat homogeneous and isotropic universe. In Secs. 3.2 and 3.3, we then consider two specific models, corresponding to two different coupling functions depending on the scalar field gradient and the fluid’s four velocity, and explore their dynamics using dynamical system techniques. In Sec. 4, we investigate the implications of these derivative coupling models in the growth of cosmological structures using linear perturbation theory within the quasi-static approximation. Finally, we draw our conclusions in Sec. 5.

Notation: In this work, we assume the $(-, +, +, +)$ signature convention for the metric. We shall adopt units where $8\pi G = c = \hbar = 1$. Moreover, the comma notation denotes standard partial derivatives (i.e. $\phi_{,\mu} = \partial_\mu\phi$).

2 Scalar-Fluid theories with a derivative coupling

2.1 The Scalar-Fluid action

The total action of scalar-fluid theories is given by [38, 39]

$$S = \int d^4x [\mathcal{L}_{\text{grav}} + \mathcal{L}_{\text{mat}} + \mathcal{L}_\phi + \mathcal{L}_{\text{int}}], \quad (2.1)$$

where $\mathcal{L}_{\text{grav}}$ stands for the gravitational Lagrangian, \mathcal{L}_{mat} stands for the matter Lagrangian, \mathcal{L}_ϕ stands for the scalar field Lagrangian and \mathcal{L}_{int} stands for the interacting Lagrangian. The gravitational Lagrangian $\mathcal{L}_{\text{grav}}$ is given by the standard Einstein-Hilbert Lagrangian

$$\mathcal{L}_{\text{grav}} = \frac{\sqrt{-g}}{2} R, \quad (2.2)$$

where g is the determinant of the metric $g_{\mu\nu}$ and R is the Ricci scalar. The matter Lagrangian \mathcal{L}_{mat} for relativistic fluid [40] is given by

$$\mathcal{L}_{\text{mat}} = -\sqrt{-g}\rho(\mathbf{n}, \mathfrak{s}) + J^\mu (\varphi_{,\mu} + \mathfrak{s}\theta_{,\mu} + \beta_A \alpha_{,\mu}^A), \quad (2.3)$$

where $\rho(\mathbf{n}, \mathfrak{s})$ is the energy density of the fluid, considered to be depending only on the particle number density \mathbf{n} and the entropy density per particle \mathfrak{s} . Here θ , φ and β_A are Lagrange multipliers with $A = 1, 2, 3$, and α_A are the Lagrangian coordinates of the fluid. The quantity J^μ , which denotes the vector density particle number, is connected to \mathbf{n} as

$$J^\mu = \sqrt{-g} \mathbf{n} u^\mu, \quad |J| = \sqrt{-g_{\mu\nu} J^\mu J^\nu}, \quad \mathbf{n} = \frac{|J|}{\sqrt{-g}}, \quad (2.4)$$

where u^μ is the fluid 4-velocity satisfying $u_\mu u^\mu = -1$. The scalar field Lagrangian \mathcal{L}_ϕ is given by the canonical form

$$\mathcal{L}_\phi = -\sqrt{-g} \left[\frac{1}{2} \partial_\mu \phi \partial^\mu \phi + V(\phi) \right], \quad (2.5)$$

where V stands for an arbitrary potential of the scalar field ϕ . Finally we consider the interacting Lagrangian term \mathcal{L}_{int} where the scalar field's first spacetime derivative $\partial_\mu \phi$ interacts with the fluid's degrees of freedom as [39]

$$\mathcal{L}_{\text{int}} = f(\mathbf{n}, \mathfrak{s}, \phi) J^\mu \partial_\mu \phi, \quad (2.6)$$

where $f(\mathbf{n}, \mathfrak{s}, \phi)$ is an arbitrary function. Note that this term represents an effective coupling between the gradient of the scalar field $\partial_\mu \phi$ and the fluid's 4-velocity u^μ as

$$\mathcal{L}_{\text{int}} = \sqrt{-g} \mathbf{n} f(\mathbf{n}, \mathfrak{s}, \phi) u^\mu \partial_\mu \phi. \quad (2.7)$$

2.2 Background cosmological equations

In what follows we shall first consider the cosmological evolution of the universe based on the action (2.1) under a spatially flat, homogeneous and isotropic Friedmann-Robertson-Walker (FRW) universe, described by the metric

$$ds^2 = -dt^2 + a^2(t)(dx^2 + dy^2 + dz^2), \quad (2.8)$$

where $a(t)$ is the scale factor depending on the cosmic time t and x, y, z are Cartesian coordinates. The cosmological equations obtained from action (2.1), are given by

$$3H^2 = \rho + \rho_\phi + \rho_{\text{int}}, \quad (2.9)$$

$$2\dot{H} + 3H^2 = -(p + p_\phi + p_{\text{int}}), \quad (2.10)$$

where $H = \frac{\dot{a}}{a}$ is the Hubble parameter and an over-dot denotes the time derivative. In the equations above, ρ and p denote the energy density and pressure of the matter fluid with

a linear EoS (EoS) w defined by $p = w\rho$ (we will mainly consider $w = 0$ in what follows, i.e. non-relativistic matter). ρ_{int} and p_{int} are the interacting energy density and pressure, while ρ_ϕ and p_ϕ are the scalar field energy density and pressure. They are respectively given by [39]

$$\rho_{\text{int}} = 0, \quad p_{\text{int}} = -\mathbf{n}^2 \frac{\partial f}{\partial \mathbf{n}} \dot{\phi}, \quad \rho_\phi = \frac{1}{2} \dot{\phi}^2 + V, \quad p_\phi = \frac{1}{2} \dot{\phi}^2 - V. \quad (2.11)$$

Finally varying action (2.1) with respect to the scalar field ϕ , we obtain the modified Klein-Gordon equation as

$$\ddot{\phi} + 3H\dot{\phi} + \frac{\partial V}{\partial \phi} - 3H\mathbf{n}^2 \frac{\partial f}{\partial \mathbf{n}} = 0. \quad (2.12)$$

Note that the Friedmann equation (2.9) does not get modified by the coupling term since $\rho_{\text{int}} = 0$; whereas the acceleration equation (2.10) and scalar field equation (2.12) are affected by the interaction.

3 Background cosmological dynamics

3.1 Formation of the autonomous system

We employ the following dimensionless variables to convert the cosmological equations (2.9)-(2.12) to an autonomous system of equations,

$$\sigma = \frac{\sqrt{\rho}}{\sqrt{3H}}, \quad x = \frac{\dot{\phi}}{\sqrt{6H}}, \quad y = \frac{\sqrt{V}}{\sqrt{3H}}, \quad s = -\frac{1}{V} \frac{dV}{d\phi}, \quad (3.1)$$

where the variable s is usually employed for arbitrary self-interacting potentials [46, 58]. Using the dimensionless variables (3.1), the Friedmann equation (2.9) becomes

$$1 = \sigma^2 + x^2 + y^2. \quad (3.2)$$

This acts as a constraint equation for the dimensionless variables (3.1), effectively decreasing the dimension of the phase space by one. The DE density parameter and the DM energy density parameter are respectively given by

$$\Omega_\phi \equiv \frac{\rho_\phi}{3H^2} = x^2 + y^2, \quad (3.3)$$

$$\Omega_m \equiv \frac{\rho}{3H^2} = 1 - x^2 - y^2. \quad (3.4)$$

Using the dimensionless variables (3.1), the cosmological equations (2.9)-(2.12) can be rewritten as the following autonomous system of equations

$$x' = -\frac{1}{2} \left[3x((w-1)x^2 + (w+1)y^2 + 1 - w) - \sqrt{6}(A(x^2 - 1) + sy^2) \right], \quad (3.5)$$

$$y' = -\frac{1}{2} y \left[3((w-1)x^2 + (w+1)(y^2 - 1)) + \sqrt{6}x(s - A) \right], \quad (3.6)$$

$$s' = -\sqrt{6} x g(s), \quad (3.7)$$

	f	A
Model I	$-\gamma \left(-\frac{1}{V} \frac{dV}{d\phi}\right)^\beta \rho^{1/2-\alpha} V^\alpha / \sqrt{3}n$	$\xi s^\beta y^{2\alpha} (1-x^2-y^2)^{1/2-\alpha}$
Model II	$\xi \left(-\frac{1}{V} \frac{dV}{d\phi}\right)^\beta \frac{H_0}{n}$	$\xi s^\beta \frac{H_0}{H}$

Table 1: Explicit expression of A (see Eq. (3.9)) for the choices of the interacting function f considered in Sec. 3.2 (Model I) and Sec. 3.3 (Model II). Here $\alpha, \beta, \gamma, \xi$ are all dimensionless parameters and γ is defined as $\gamma = \xi / [(\frac{1}{2} - \alpha)(w + 1) - 1]$.

where $g(s) = s^2(\Gamma(s) - 1)$ and

$$\Gamma = V \frac{d^2V}{d\phi^2} \left(\frac{dV}{d\phi} \right)^{-2}, \quad (3.8)$$

while a prime denotes differentiation with respect to the number of e -folds N defined by $dN = H dt$. In Eqs. (3.5)-(3.7), we have also introduced the dimensionless quantity

$$A = -\frac{1}{H} \mathbf{n}^2 \frac{\partial f}{\partial \mathbf{n}}. \quad (3.9)$$

Different types of scalar field potential $V(\phi)$ lead to different forms of Γ , with the exponential potential being the simplest possible choice ($\Gamma = 1$). In what follows we will assume that Γ can always be written as a function of s . This assumption holds for a wide class of scalar field potential, including many of the cases considered in cosmology (see e.g. [58]). In order to close the system, we must also specify the coupling function f from which A can be obtained. For some choices of f , the quantity A depends solely on x, y and s and the resulting system remains autonomous. However in the most general situation A cannot be written as a function of x, y and s only, and an extra variable must be introduced, increasing in this way the dimension of the system. In what follows, we consider the two choices of f given in Table 1, referring to them as Model I and Model II. They generalise the cases considered in [39]. In Model I, the quantity A depends solely on x, y and s , while in Model II it cannot be written in terms of x, y and s only and a further variable must be introduced (see Sec. 3.3).

3.2 Model I

This section deals with the phase space analysis of the dynamical system (3.5)-(3.7) for Model I. In terms of the dimensionless variables (3.1), the acceleration equation (2.10) can be expressed as

$$\frac{\dot{H}}{H^2} = \frac{3}{2} \left\{ -(1+w) + (w-1)x^2 + (w+1)y^2 - \sqrt{\frac{2}{3}} x \xi s^\beta y^{2\alpha} (1-x^2-y^2)^{1/2-\alpha} \right\}. \quad (3.10)$$

This implies that the effective EoS parameter w_{eff} can be written as

$$\begin{aligned} w_{\text{eff}} &\equiv \frac{p + \frac{1}{2}\dot{\phi}^2 - V + p_{\text{int}}}{\rho + \frac{1}{2}\dot{\phi}^2 + V + \rho_{\text{int}}} \\ &= x^2 - y^2 + w(1-x^2-y^2) + \sqrt{\frac{2}{3}} x \xi s^\beta y^{2\alpha} (1-x^2-y^2)^{1/2-\alpha}. \end{aligned} \quad (3.11)$$

Model I	$\beta = 0$	$\alpha = 0$
		$\alpha = 1/2$
	$\beta = 1$	$\alpha = 0$
		$\alpha = 1/2$
Model II	$\beta = 0$	–
	$\beta = 1$	–

Table 2: Choices of α and β considered in this paper for both Model I and II (see Table 1).

Point	x	y	s	Existence	w_{eff}
$A_{1\pm}$	± 1	0	s_*	Always	1
A_2	$\frac{s_*}{\sqrt{6}}$	$\sqrt{1 - \frac{s_*^2}{6}}$	s_*	$s_*^2 \leq 6$	$\frac{s_*^2 - 3}{3}$
A_3	$-\sqrt{\frac{2}{3(w-1)^2 + 2\xi^2}} \xi$	0	s_*	Always	$\frac{3w}{3+2\xi^2}$
A_4	0	1	0	Always	–1

Table 3: Critical points of $(0, 0)$ model (Sec. 3.2.1).

The physically meaningful assumption $\rho \geq 0$, namely $\sigma^2 \geq 0$, implies that one obtains from the constraint equation (3.2) the condition

$$x^2 + y^2 \leq 1. \quad (3.12)$$

Hence, the three dimensional phase space of the system (3.5)-(3.7) for Model I is given by

$$\Psi = \{(x, y) \in \mathbb{R}^2 : 0 \leq x^2 + y^2 \leq 1\} \times \{s \in \mathbb{R}\}. \quad (3.13)$$

Note also that whenever α is an integer number the dynamical system (3.5)-(3.7) is invariant under the transformation $y \mapsto -y$, implying that the dynamics for $y > 0$ can be mirrored into the dynamics for $y < 0$.

Model I becomes singular whenever $y = 0$, $\sigma = 0$ or $s = 0$ for all values of α , β except in the range $0 \leq \alpha \leq \frac{1}{2}$ and $\beta \geq 0$. For this reason we will restrict our study only to values of α and β belonging to this range. In general it is difficult to perform a complete dynamical system analysis for arbitrary values of α and β , so in what follows we will investigate the background cosmological dynamics only for the specific choices of α and β reported in Table 2. We shall denote a particular model with given β and α by (β, α) . For example, the model with $\beta = 1$, $\alpha = 0$ will be denoted as the $(1, 0)$ model. The background cosmological dynamics for the $(0, \frac{1}{2})$ model coincides with the one obtained by the k -essence scalar field studied in [47, 60], and for this reason it will not be present again here.

3.2.1 $(0, 0)$ model

The critical points of the system (3.5)-(3.7) for this particular model are given in Table 3 and their corresponding eigenvalues along with their stability criteria are given in Table 4. In what follows, s_* represents the solution of equation $g(s) = 0$ and $dg(s_*)$ is the derivative of g at $s = s_*$. The system has five critical points depending on s_* and ξ . Critical points $A_{1\pm}$, A_2 , A_3 depend on the concrete form of the scalar field potential through s_* , whereas

$$\text{Here: } \Delta = \sqrt{\frac{3}{3(1-w)^2 + 2\xi^2}}$$

Point	λ_1	λ_2	λ_3	Stability
$A_{1\pm}$	$3(1-w)$	$3 \mp \frac{\sqrt{6}s_*}{2}$	$\mp\sqrt{6} dg(s_*)$	Unstable node/Saddle.
A_2	$\frac{s_*^2}{2} - 3$	$s_*^2 - 3(w+1)$	$-s_* dg(s_*)$	Stable node if $s_*^2 < 3(w+1)$, $s_* dg(s_*) > 0$ Saddle node otherwise
A_3	$\frac{3}{2}(w-1)$	$\frac{3}{2}(w+1) + \Delta s_* \xi$	$2\Delta \xi dg(s_*)$	Stable node if $s_* \xi < -\frac{3}{2}(w+1)\sqrt{(1-w)^2 + \frac{2\xi^2}{3}}$, $\xi dg(s_*) < 0$ Saddle node otherwise
A_4	$-3(w+1)$	$-\frac{3}{2}\left(1 + \sqrt{1 - \frac{4}{3}g(0)}\right)$	$-\frac{3}{2}\left(1 - \sqrt{1 - \frac{4}{3}g(0)}\right)$	Stable if $g(0) > 0$ Saddle if $g(0) < 0$

Table 4: Stability of critical points of $(0, 0)$ model (Sec. 3.2.1).

critical point A_4 corresponds to the case where the potential is effectively constant. Note that critical point A_2 reduces to point A_4 when $s_* = 0$. The properties of the critical points are the following:

- Points $A_{1\pm}$ exist for any values of s_* and ξ . They correspond to a decelerated solution dominated by the kinetic energy of the scalar field, with stiff fluid effective EoS ($w_{\text{eff}} = 1$). Points $A_{1\pm}$ are unstable node whenever $\pm s_* < \sqrt{6}$ and $\pm dg(s_*) < 0$, otherwise they are saddle.
- Point A_2 exists for $s_*^2 \leq 6$. It corresponds to a scalar field dominated solution. It also corresponds to an accelerated universe when $s_*^2 < 2$. It is a stable node if $s_*^2 < 3(w+1)$ and $s_* dg(s_*) > 0$, otherwise it is a saddle.
- Point A_3 exists for any values of ξ and s_* . It corresponds to a decelerated solution where the energy content of the universe is shared between matter and the kinetic energy of the scalar field. It is a stable node if $s_* \xi < -\frac{3}{2}(w+1)\sqrt{(1-w)^2 + \frac{2\xi^2}{3}}$ and $\xi dg(s_*) < 0$, otherwise it is a saddle.
- Point A_4 corresponds to an accelerated, scalar field dominated solution with $w_{\text{eff}} = -1$. It is a stable node whenever $0 < g(0) < \frac{3}{4}$, it is stable spiral when $g(0) > \frac{3}{4}$ and saddle whenever $g(0) < 0$. For $g(0) = 0$ linear theory fails to determine its stability, and other mathematical tools, as e.g. center manifold theory, or numerical techniques should be employed. In these cases the stability of point A_4 can be determined numerically once a specific potential has been chosen. For example we have numerically checked that for some phenomenologically interesting potentials, such as for example $V = \frac{M^{4+n}}{\phi^n}$ (with M and $n > 0$ constants), point A_4 is stable.

From this analysis, we observe that depending on the choice of the scalar field potential, on the choice of the parameter ξ , as well as on the initial conditions, the universe evolves from a stiff matter dominated solution (points $A_{1\pm}$) either towards a decelerated scaling solution (point A_3), or towards an accelerated, scalar field dominated solution (points A_2 or A_4). The standard matter dominated solution of the canonical scalar field model is replaced by point

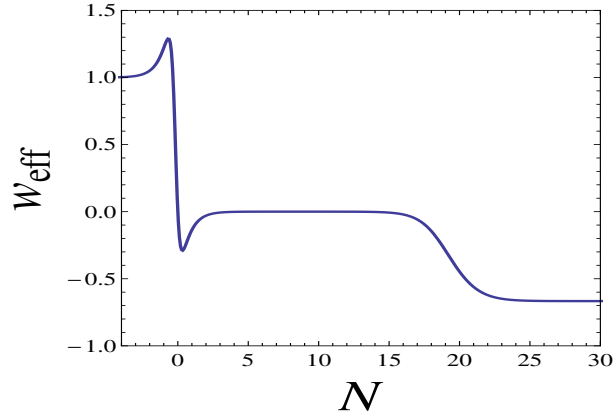


Figure 1: Plot of w_{eff} versus N for $(0,0)$ model. Here we have considered the potential $V = V_0 \sinh^{-\eta}(\mu\phi)$ with $w = 0$, $\xi = -1.5$, $\eta = 1$ and $\mu = 1$.

$$\text{Here: } \Delta = \sqrt{\xi^2 s_*^2 ((\xi^2 + 4) s_*^2 - 12(w + 1))}, \quad x_2 = \sqrt{\frac{2}{2\xi^2 s_*^2 + 3(1-w)^2}},$$

$$\Xi = \frac{1}{2} \xi \frac{\sqrt{2 s_*^2 (\xi^2 + 2) - 2\Delta - 12w - 12s_* (w+1) + s_*^2 \xi^2 (w+1) + 2 s_*^2 w - \Delta(w+1)}}{s_*^2}$$

Point	x	y	s	Existence	w_{eff}
C_0	0	0	0	Always	w
$C_{1\pm}$	± 1	0	s_*	Always	1
C_2	x_2	0	s_*	Always	w
C_3	$\frac{1}{2} \frac{\sqrt{6}(w+1)}{s_*}$	$\frac{\sqrt{3(1-w^2) - s_*^2 \xi^2 + \Delta}}{\sqrt{2} s_*}$	s_*	Fig. 2	Ξ
C_4	$\frac{s_*}{\sqrt{6}}$	$\sqrt{1 - \frac{s_*^2}{6}}$	s_*	$s_*^2 < 6$	$-1 + \frac{s_*^2}{3}$
C_5	0	1	0	Always	-1

Table 5: Critical points of $(1,0)$ model (Sec. 3.2.2).

A_3 , which is not a matter dominated solution but has $w_{\text{eff}} = 0$ for $w = 0$, i.e. it behaves as if the universe was matter dominated even though $\Omega_m \neq 1$. This feature appears also for canonical scalar field DE models coupled to the matter sector [22]. Moreover, point A_3 can become the late time attractor, unlike the matter dominated solution of the canonical scalar field model. This model can thus be used to describe the late time transition of our universe from a DM effective behavior (point A_3) to DE domination (points A_2 or A_4). Note that point A_2 can be a late time accelerating scaling solution (see Fig. 1 for an example), which can be used to alleviate the cosmic coincidence problem.

3.2.2 $(1,0)$ model

This section deals with the phase space analysis of the dynamical system (3.5)-(3.7) for the choices of $\beta = 1$ and $\alpha = 0$. In terms of dimensionless variables (3.1), the effective EoS

Here: $\eta_{\pm} = -3 + \frac{3}{4}s_*^2 - \frac{3}{2}w \pm \frac{1}{4}\sqrt{-4s_*^4\xi^2 + s_*^4 + 24s_*^2\xi^2 - 12s_*^2w + 36w^2}$

Point	λ_1	λ_2	λ_3	Stability
C_0	$\frac{3}{2}(1+w)$	$-\frac{3(1-w)}{4}\left(1 - \sqrt{\frac{16}{3}\frac{g(0)\xi}{(1-w)} + 1}\right)$	$-\frac{3(1-w)}{4}\left(1 + \sqrt{\frac{16}{3}\frac{g(0)\xi}{(1-w)} + 1}\right)$	Saddle
$C_{1\pm}$	$3(1-w)$	$3 \mp \sqrt{\frac{3}{2}}s_*$	$\mp\sqrt{6}dg(s_*)$	Unstable node/ Saddle
C_2	$-\frac{3}{2}(1-w)$	$\frac{3}{2}(w+1) - \sqrt{\frac{3}{2}}s_*^2\xi x_2$	$-\sqrt{6}x_2\xi s_* dg(s_*)$	Stable node/Saddle
C_3	-	-	$-\frac{3(w+1)dg(s_*)}{s_*}$	Fig. 2
C_4	η_+	η_-	$-s_* dg(s_*)$	Fig. 2
C_5	$-3(w+1)$	$-\frac{3}{2}\left(1 + \sqrt{1 - \frac{4g(0)}{3}}\right)$	$-\frac{3}{2}\left(1 - \sqrt{1 - \frac{4g(0)}{3}}\right)$	Saddle if $g(0) < 0$ Stable if $g(0) > 0$ See Appendix A.2 if $g(0) = 0$

Table 6: Stability of critical points listed in Table 5. The expressions for the eigenvalues of point C_3 have not been written due to their excessive length.

parameter w_{eff} is given by

$$w_{\text{eff}} = x^2 - y^2 + w(1 - x^2 - y^2) + \sqrt{\frac{2}{3}}x\xi s(1 - x^2 - y^2)^{1/2}. \quad (3.14)$$

The critical points of the system (3.5)-(3.7) for this model are given in Table 5 and their corresponding eigenvalues along with their stability criteria are given in Table 6. The system has six critical points depending on the values of s_* and ξ . All critical points depend on the concrete form of the potential $V(\phi)$ through s_* . Points C_0 and C_5 correspond to the case where the variable $s = 0$, i.e. when the potential is effectively constant. The properties of the critical points are as follow:

- Point C_0 corresponds to a matter dominated solution ($\Omega_m = 1$) with effective EoS parameter coinciding with the matter one ($w_{\text{eff}} = w$). It is always saddle.
- Points $C_{1\pm}$ exist for any values of s_* and ξ . They correspond to a decelerated solution dominated by the kinetic energy of the scalar field, with stiff fluid effective EoS ($w_{\text{eff}} = 1$). Point $C_{1\pm}$ are unstable nodes whenever $\pm s_* < \sqrt{6}$ and $\pm dg(s_*) < 0$, otherwise they are saddle.
- Point C_2 corresponds to a decelerated scaling solutions with effective EoS mimicking a matter era: $w_{\text{eff}} = w$. It is stable when $\xi > \sqrt{\frac{3}{2}}\frac{(w+1)}{s_*^2 x_2}$ and $\xi s_* dg(s_*) > 0$, otherwise it is saddle.
- Due to the complicated expressions of point C_3 , we numerically determine its regions of existence and stability in the (s_*, ξ) parameter space assuming $w = 0$ (see Fig. 2). In the same figure we report the regions of parameter space where point C_3 can describe a late time accelerated scaling solution.
- Point C_4 corresponds to a scalar field dominated solution. It exists whenever $s_*^2 < 6$ and describes an accelerated universe if $s_*^2 < 2$. It reduces to the critical point C_5 for $s_* = 0$.

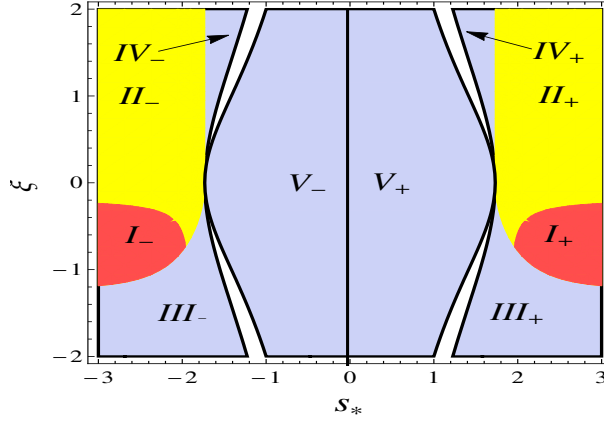


Figure 2: Existence and stability regions of points C_3, C_4 on the (s_*, ξ) parameter space. Regions $I_+, I_-, II_+, II_-, III_+, III_-, IV_+, IV_-$ represent regions of existence of point C_3 . Regions I_+ and II_+ represent regions of stability of point C_3 for potentials where $dg(s_*) > 0$ and regions I_- and II_- represent its regions of stability for potentials where $dg(s_*) < 0$. Red shaded regions (i.e. regions I_+ and I_-) represent regions of acceleration for point C_3 . Region V_+ represents the region of stability of point C_4 for potential with $dg(s_*) > 0$ and region V_- represents its region of stability for potential with $dg(s_*) < 0$. Here we have taken $w = 0$.

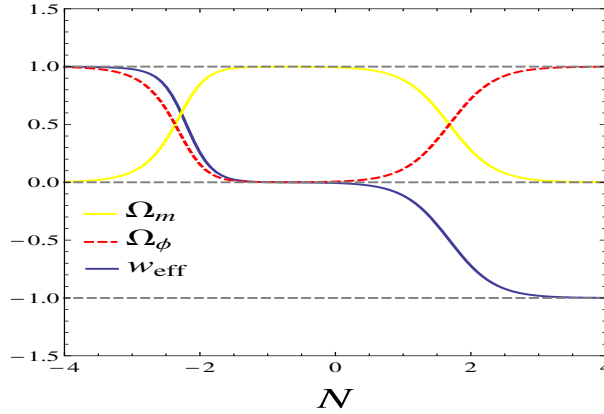


Figure 3: Plot of Ω_m, Ω_ϕ and w_{eff} versus N for $(1, 0)$ model. Here we have considered the potential $V = V_0 \sinh^{-\eta}(\mu\phi)$ with $w = 0, \alpha = 0, \xi = -1.5, \eta = -1$ and $\mu = 1$.

The stability conditions of this point are again determined numerically by plotting the regions of stability in the (s_*, ξ) parameter space (see Fig. 2).

- Point C_5 corresponds to an accelerated scalar field dominated solution with effective EoS $w_{\text{eff}} = -1$. It is a saddle if $g(0) < 0$, while it represents a late time attractor if $g(0) > 0$. If $g(0) = 0$, linear stability fails. In this case we use center manifold theory to determine its stability. The detailed analysis using these advanced tools is presented in appendix A.2. From that analysis, we find that point C_5 is always unstable unless $dg(0) = 0$.

From the analysis of the critical points, we understand that, depending on the choice of the potential $V(\phi)$, of the parameter ξ , as well as the initial conditions, the universe can

$$\text{Here: } \Delta = \sqrt{\xi^2 s_*^2 + 6(1-w^2)}, \Xi_4 = \frac{2\xi^2 s_*^4 - 3\xi^2 s_*^2 - 2s_*^4 + 12s_*^2 - 18}{2\xi^2 s_*^4}$$

Point	x	y	s	Existence	w_{eff}
D_0	0	0	s	Always	w
$D_{1\pm}$	± 1	0	s_*	Always	1
$D_{2\pm}$	$\frac{1}{2} \frac{\sqrt{6(w+1)}}{s_*}$	$\frac{\xi s_* \pm \Delta}{2s_*}$	s_*	$0 \leq (\xi s_* \pm \Delta)^2 + 6(w+1) \leq 4s_*^2$	w
D_3	$\frac{s_* (\xi \sqrt{\xi^2 s_*^2 - s_*^2 + 6} + \sqrt{6})}{(\xi^2 s_*^2 + 6)}$	$-\frac{\sqrt{6(\xi^2 s_*^2 - s_*^2 + 6)} - \xi s_*^2}{\xi^2 s_*^2 + 6}$	s_*	Always	$-\frac{-\xi \sqrt{\xi^2 s_*^2 - s_*^2 + 6} \sqrt{6s_*^2 + 3(\xi^2 s_*^2 - 2s_*^2 + 6)}}{3(\xi^2 s_*^2 + 6)}$
D_4	$\frac{\sqrt{6}}{2s_*}$	$\frac{s_*^2 - 3}{\xi s_*^2}$	s_*	$0 \leq \frac{3\xi^2 s_*^2 + 2s_*^4 - 12s_*^2 + 18}{2\xi^2 s_*^4} \leq 1$	Ξ_4
$D_{5\pm}$	0	± 1	0	Always	-1

Table 7: Critical points of $(1, \frac{1}{2})$ model (Sec. 3.2.3).

$$\text{Here: } \xi_{1\pm} = -\frac{1}{4}(1-w) \pm \frac{1}{3s_*} \left(12\xi^4 s_*^4 + 12\xi^2 \Delta \xi s_* (\xi^2 s_*^2 + s_*^2 + 3w^2 + 3w + 6) - 12\xi^2 s_*^4 - 72\xi^2 s_*^2 w^2 + 36\xi^2 s_*^2 w + 108\xi^2 s_*^2 + 81s_*^2 w^2 - 18ws_*^2 - 63s_*^2 + 216(w+1)(1-w^2) \right)^{\frac{1}{2}}$$

$$\xi_{2\pm} = -\frac{1}{4}(1-w) \pm \frac{1}{3s_*} \left(12\xi^4 s_*^4 + 12\xi^2 \Delta \xi s_* (\xi^2 s_*^2 + s_*^2 + 3w^2 + 3w + 6) - 12\xi^2 s_*^4 - 72\xi^2 s_*^2 w^2 + 36\xi^2 s_*^2 w + 108\xi^2 s_*^2 + 81s_*^2 w^2 - 18ws_*^2 - 63s_*^2 + 216(w+1)(1-w^2) \right)^{\frac{1}{2}}$$

Point	λ_1	λ_2	λ_3	Stability
D_0	0	$-\frac{3}{2}(1-w)$	$\frac{3}{2}(1+w)$	Saddle.
$D_{1\pm}$	$3(1-w)$	$3\mp \sqrt{\frac{3}{2}} s_*$	$\mp \sqrt{6} dg(s_*)$	Unstable node/ Saddle
$D_{2\pm}$	$\xi_{1\pm}$	$\xi_{2\pm}$	$-\frac{3(w+1)}{s_*} dg(s_*)$	Fig. 4
D_3	$-\frac{-\xi \sqrt{6(\xi^2 s_*^2 - s_*^2 + 6)} s_*^2 + 3(\xi^2 s_*^2 - 2s_*^2 + 6)}{\xi^2 s_*^2 + 6}$	$-\frac{-\xi \sqrt{6(\xi^2 s_*^2 - s_*^2 + 6)} s_*^2 + 6(\xi^2 s_*^2 - s_*^2 + 6)}{2(\xi^2 s_*^2 + 6)}$	$-\frac{\sqrt{3s_*} (\xi \sqrt{2\xi^2 s_*^2 - 2s_*^2 + 12 + 2\sqrt{3}}) dg(s_*)}{\xi^2 s_*^2 + 6}$	Fig. 5
D_4	$\frac{3(2\xi^2 s_*^4 - 2s_*^4 - 3\xi^2 s_*^2 + 12s_*^2 - 18)}{4\xi^2 s_*^4}$	$\frac{3(4\xi^2 s_*^4 - 6s_*^4 - 9\xi^2 s_*^2 + 36s_*^2 - 54)}{4\xi^2 s_*^4}$	$-\frac{3dg(s_*)}{s_*}$	Unstable node/ Saddle
$D_{5\pm}$	$-3(w+1)$	$-\frac{3}{2} + \frac{1}{2}\sqrt{9-12g(0)(1\mp\xi)}$	$-\frac{3}{2} - \frac{1}{2}\sqrt{9-12g(0)(1\mp\xi)}$	Saddle if $g(0)(1\mp\xi) < 0$ Stable if $g(0)(1\mp\xi) > 0$ See Appendix A.2 if $g(0)(1\mp\xi) = 0$

Table 8: Stability of critical points listed in Table 7. Points D_3 and D_4 are analysed only for $w = 0$.

evolve from a stiff matter dominated solution (points $C_{1\pm}$) either towards an accelerated scaling solution C_3 , or towards an accelerated, scalar field dominated solution (points C_4 or C_5), passing through a long lasting matter dominated solution (point C_0) or a decelerated scaling solution (point C_2) with $w_{\text{eff}} = w$. This means that the $(1, 0)$ model can be used to describe the observed transition of the universe from a matter dominated era to a late time DE dominated era (see Fig. 3 for an example). Moreover the background dynamics of this model presents different scaling solutions (points C_2 , C_3 and C_4) which can be used to obtain interesting phenomenology: for example late time accelerated scaling solutions can be used to alleviate the cosmic coincidence problem and scaling solutions mimicking a matter era could present interesting observational signatures at the perturbation level without affecting the background dynamics (see Sec. 4).

3.2.3 $(1, \frac{1}{2})$ model

This section deals with the phase space analysis of the dynamical system (3.5)-(3.7) for $\beta = 1$ and $\alpha = \frac{1}{2}$. In terms of the dimensionless variables (3.1), the effective EoS parameter w_{eff} is given by

$$w_{\text{eff}} \equiv \frac{p + \frac{1}{2}\dot{\phi}^2 - V + p_{\text{int}}}{\rho + \frac{1}{2}\dot{\phi}^2 + V + \rho_{\text{int}}} = x^2 - y^2 + w(1 - x^2 - y^2) + \sqrt{\frac{2}{3}} \xi s x y \quad (3.15)$$

The critical points of the system (3.5)-(3.7) are given in Table 7 and their corresponding eigenvalues along with their stability criteria are given in Table 8. The system presents nine critical points depending on s_* and ξ . Note that critical point D_3 reduces to point D_{5-} when $s_* = 0$. The properties of these critical points are the following:

- Point D_0 is independent of the specific scalar field potential under considerations for its existence. It corresponds to a matter dominated solution with $w_{\text{eff}} = w$. It always behaves as a saddle.
- Points $D_{1\pm}$ exist for any values of s_* and ξ . They correspond to a decelerated solution dominated by the kinetic energy of the scalar field, with stiff fluid effective EoS ($w_{\text{eff}} = 1$). Points $D_{1\pm}$ are unstable node whenever $\pm s_* < \sqrt{6}$ and $\pm dg(s_*) < 0$, otherwise they are saddle.
- Points $D_{2\pm}$ correspond to decelerated scaling solutions with effective EoS mimicking a matter era ($w_{\text{eff}} = w$). The stability condition for points $D_{2\pm}$ cannot be determined analytically due to the complicated expressions of their eigenvalues. However they can be stable for some values of s_* and ξ , as checked numerically and shown in Fig. 4 by plotting their regions of existence and stability in the (s_*, ξ) parameter space for $w = 0$. In any case since they always constitute decelerated solutions, these points cannot describe the late time acceleration of the universe.
- Due to the extremely complicated expressions associated to point D_3 , we are able to determine its stability only fixing the parameter w . For this purpose we choose $w = 0$. In this case point D_3 exists for any values s_* and ξ . It corresponds to a late accelerated scalar field dominated solution ($\Omega_\phi = 1$) for some values of s_* and ξ (see Fig. 5).
- Point D_4 is again analysed only for the $w = 0$ case due to the complicated expressions associated to it. It exists for $0 \leq \frac{3\xi^2 s_*^2 + 2s_*^4 - 12s_*^2 + 18}{2\xi^2 s_*^4} \leq 1$. Numerically we have checked that this point is not stable within its region of existence: it is either saddle or an unstable node.
- Points $D_{5\pm}$ correspond to accelerated, scalar field dominated solutions with $w_{\text{eff}} = -1$. Point D_{5-} is a special case of point D_3 for $s_* = 0$. Point D_{5+} is a saddle if $g(0)(1-\xi) < 0$, it is stable if $g(0)(1-\xi) > 0$ but linear stability fails to determine the stability if $g(0)(1-\xi) = 0$. Similarly, point D_{5-} is a saddle if $g(0)(1+\xi) < 0$, it is stable if $g(0)(1+\xi) > 0$ and linear stability fails to determine the stability if $g(0)(1+\xi) = 0$, in which case other mathematical tools, as for example center manifold theory, are required to complete the analysis. The complete investigation using center manifold techniques for point D_{5-} and D_{5+} is reported in appendix A.2. From its results we find that points $D_{5\pm}$ are always unstable unless $dg(0)(1 \mp \xi) = 0$.

From the analysis of the critical points, it can be observed that the universe evolves from an early-time stiff matter dominated solutions $D_{1\pm}$ towards an accelerated, scalar field dominated solution (points $D_3, D_{5\pm}$), possibly passing through a long lasting matter dominated solution D_0 (or $D_{2\pm}$). This model can thus used to phenomenologically describe the observed transition of the universe from a matter dominated era to a late time DE dominated era (see Fig. 6 for an example). Moreover points $D_{2\pm}$ describe scaling solutions which can be used to characterize a matter era with $w_{\text{eff}} = w$. Since for these solutions the energy density of the scalar field does not vanish, some deviations from standard Λ CDM dynamics might be

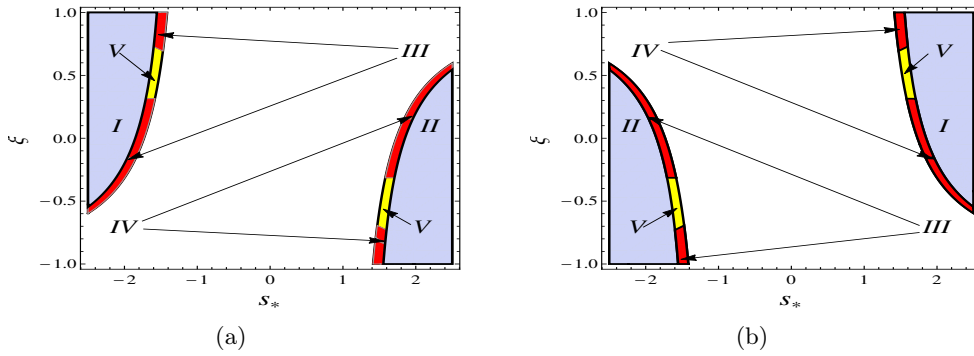


Figure 4: Existence and stability regions of point D_{2+} (a) and point D_{2-} (b) on the (s_*, ξ) parameter space. In both panels, the whole shaded regions represent regions of existence. Regions I and II represent regions where the point is a stable spiral for potentials giving $dg(s_*) < 0$ and $dg(s_*) > 0$, whereas regions III and IV represent regions where the point is a stable node for potentials giving $dg(s_*) < 0$ and $dg(s_*) > 0$ respectively. Yellow shaded region V represents the region where the point is saddle. Here we have assumed $w = 0$.

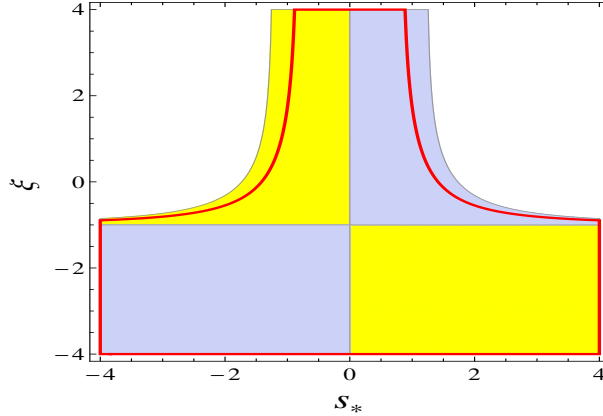


Figure 5: Existence and stability regions of point D_3 on the (s_*, ξ) parameter space. The yellow shaded regions represent regions of stability of the point for potentials giving $dg(s_*) < 0$, whereas blue shaded regions represent regions of stability of the point for potentials giving $dg(s_*) > 0$. Region enclosed inside the red colored boundary corresponds to the region of acceleration.

present at the perturbation level, even if the background evolution is undistinguishable (see Sec. 4).

3.3 Model II

In this section we present the phase space analysis of the system (3.5)-(3.7) for Model II (see Table 1), where the coupling function f is of the form $\xi \left(-\frac{1}{V} \frac{dV}{d\phi} \right)^\beta \frac{H_0}{\kappa \Pi}$, with ξ a constant and H_0 the Hubble constant. It can be seen from Table 1 that the quantity A does not depend solely on x, y, s and hence, as discussed previously, another extra variable z is required to close the autonomous system (3.5)-(3.7). In what follows we will choose this further variable

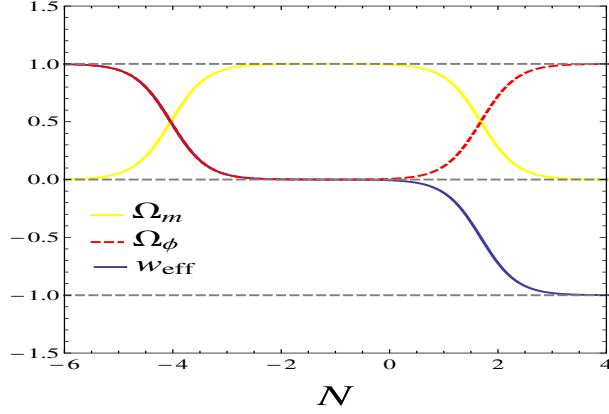


Figure 6: Evolution of Ω_ϕ , Ω_m and w_{eff} versus N for $(1, \frac{1}{2})$ model. Here we considered a potential $V = V_0 \sinh^{-\eta}(\mu\phi)$ with $\eta = -1$, $\mu = 1$, $w = 0$ and $\xi = 1$.

as

$$z = \frac{H_0}{H + H_0}, \quad (3.16)$$

which is bounded as $0 \leq z \leq 1$. The dynamical system (3.5)-(3.7) becomes then

$$x' = -\frac{1}{2(z-1)} \left[3x(z-1) (1-w + (w-1)x^2 + (1+w)y^2) + \sqrt{6} \left(-\xi s^\beta z(1-x^2) - s(z-1)y^2 \right) \right], \quad (3.17)$$

$$y' = -\frac{y}{2(z-1)} \left[3(z-1) \left((1+w)(y^2-1) + (w-1)x^2 \right) + \sqrt{6}x \left((z-1)s + z\xi s^\beta \right) \right], \quad (3.18)$$

$$z' = \frac{z}{2} \left[3(z-1) \left((1+w)(y^2-1) + (w-1)x^2 \right) + \sqrt{6}z\xi s^\beta \right], \quad (3.19)$$

$$s' = -\sqrt{6}xg(s). \quad (3.20)$$

The four dimensional phase space of the system (3.17)-(3.20) is given by

$$\Psi = \{(x, y, z) \in \mathbb{R}^3 : 0 \leq x^2 + y^2 \leq 1, 0 \leq z \leq 1\} \times \{s \in \mathbb{R}\}. \quad (3.21)$$

The acceleration equation (2.10) for this coupling model yields

$$\frac{\dot{H}}{H^2} = \frac{3}{2} \left\{ -(w+1) - (1-w)x^2 + (w+1)y^2 - \frac{2s^\beta \xi}{\sqrt{6}} \frac{zx}{(1-z)} \right\}. \quad (3.22)$$

Hence, the effective EoS parameter is given by

$$w_{\text{eff}} = w + (1-w)x^2 - (w+1)y^2 + \frac{2s^\beta \xi}{\sqrt{6}} \frac{zx}{(1-z)} \quad (3.23)$$

Here will investigate only the cases $\beta = 0$ and $\beta = 1$ (cf. Table 2), since the complete analysis with a general β would be too complicated.

Point	x	y	z	s	Existence	w_{eff}
E_0	0	0	0	s	Always	w
$E_{1\pm}$	± 1	0	0	s_*	Always	1
E_2	$\sqrt{\frac{3}{2}} \frac{(1+w)}{s_*}$	$\sqrt{\frac{3}{2}} \frac{\sqrt{(1+w)(1-w)}}{s_*}$	0	s_*	Always	w
E_3	$\frac{s_*}{\sqrt{6}}$	$\sqrt{1 - \frac{s_*^2}{6}}$	0	s_*	$s_*^2 \leq 6$	$\frac{s_*^2}{3} - 1$
E_4	0	1	$\frac{s_* + \xi}{s_* + \xi}$	s_*	$0 \leq \frac{s_*}{s_* + \xi} \leq 1$	-1
$E_{5\pm}$	± 1	0	$\frac{\sqrt{6}}{\sqrt{6 \mp \xi}}$	s_*	$\pm \xi < 0$	-1
E_6	0	1	0	0	Always	-1

Table 9: Critical points of Model II with $\beta = 0$ (Sec. 3.3.1).

$$\Xi_{\pm} = -\frac{3}{4}(1-w) \pm \frac{3}{4s_*} \sqrt{(1-w)(24(1+w)^2 - s_*^2(7+9w))}$$

Point	λ_1	λ_2	λ_3	λ_4	Stability
E_0	0	$\frac{3}{2}(w-1)$	$\frac{3}{2}(w+1)$	$\frac{3}{2}(w+1)$	Saddle
$E_{1\pm}$	$3(1-w)$	$3 \mp \frac{\sqrt{6}}{2}s_*$	3	$\mp \sqrt{6} dg(s_*)$	Unstable node/saddle
E_2	$\frac{3}{2}(1+w)$	Ξ_+	Ξ_-	$-\frac{3(w+1)dg(s_*)}{s_*}$	Saddle
E_3	$\frac{s_*^2-6}{2}$	$\frac{s_*^2}{2}$	$s_*^2 - 3(1+w)$	$-s_* dg(s_*)$	Saddle
E_4	$-3(1+w)$	$-\frac{3}{2} \left(1 + \sqrt{1 - \frac{2s_*^2}{3}}\right)$	$-\frac{3}{2} \left(1 - \sqrt{1 - \frac{2s_*^2}{3}}\right)$	0	-
$E_{5\pm}$	-3	$-3(w+1)$	$\mp \frac{\sqrt{6}}{2}s_*$	$\mp \sqrt{6} dg(s_*)$	Stable node if $\pm s_* > 0, \pm dg(s_*) > 0$ Saddle otherwise
E_6	0	$-3(w+1)$	$-\frac{3}{2} \left(1 + \sqrt{1 - \frac{4}{3}g(0)}\right)$	$-\frac{3}{2} \left(1 - \sqrt{1 - \frac{4}{3}g(0)}\right)$	Saddle if $g(0) < 0$ See Appendix A.2 for $g(0) \geq 0$

Table 10: Stability of critical points given in table 9.

3.3.1 $\beta = 0$ case

The critical points of the system (3.17)-(3.20) for the choice $\beta = 0$ are given in Table 9 and their corresponding eigenvalues along with their stability criteria are given in Table 10. The system has nine critical points depending on s_* and ξ . Critical points $E_{1\pm}$, E_2 , E_3 , E_4 and $E_{5\pm}$ depend on the concrete form of the potentials $V(\phi)$ through s_* . Note that critical points E_3 and E_4 reduce to point E_6 when $s_* = 0$. The properties of the critical points are:

- Point E_0 exists for any scalar field potential. It corresponds to a decelerated matter dominated solution with $w_{\text{eff}} = w$ and it always behaves as a saddle.
- Points $E_{1\pm}$ exist for any values of ξ and s_* . They correspond to stiff matter solutions ($w_{\text{eff}} = 1$), dominated by the kinetic part of the scalar field. Point $E_{1\pm}$ are unstable nodes when $\pm s_* < \sqrt{6}$ and $\pm dg(s_*) < 0$, otherwise they are saddle.
- Point E_2 exists for any values of ξ and s_* . It corresponds to a decelerated scaling solution with $w_{\text{eff}} = w$. It is always saddle since the eigenvalues of the Jacobian matrix always satisfy $\lambda_1 > 0$ and $\lambda_3 < 0$.
- Point E_3 exists for $s_*^2 \leq 6$. It always corresponds to a scalar field dominated universe and describes an accelerated universe if $s_*^2 < 2$. It is a saddle for any values of ξ and

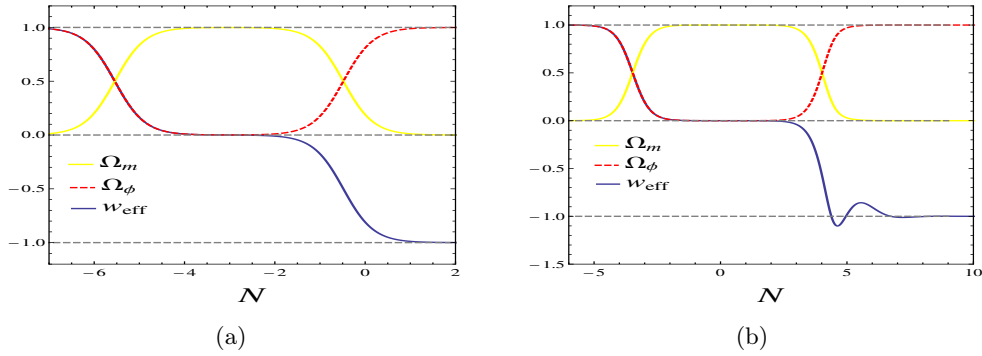


Figure 7: Plot of Ω_m , Ω_ϕ , w_{eff} versus N of model II with potential $V = V_0 \sinh^{-\eta}(\mu\phi)$. In both panels we have taken $w = 0$, $\xi = 10$, $\mu = 1$, $\eta = 2$, $\beta = 0$ with different initial conditions.

s_* since at least two of its corresponding eigenvalues have opposite sign: $\lambda_1 < 0$ and $\lambda_2 > 0$.

- Point E_4 exists when $0 \leq \frac{s_*}{s_* + \xi} \leq 1$ and it characterizes a universe dominated by the scalar field potential energy, and consequently $w_{\text{eff}} = -1$. Since it is a non-hyperbolic point ($\lambda_4 = 0$), we cannot determine its stability properties using linear stability theory. This point has to be analysed using center manifold theory or numerical techniques only once a specific potential has been selected. We have anyway checked that for some phenomenologically relevant scalar field potentials this point can be stable.
- Points $E_{5\pm}$ exist when $\mp\xi < 0$. They correspond to an accelerated universe mimicking a cosmological constant EoS ($w_{\text{eff}} = -1$), and are dominated by the scalar field kinetic energy. Point E_{5+} is a stable node when $s_* > 0$ and $dg(s_*) > 0$, whereas point E_{5-} is a stable node when $s_* < 0$ and $dg(s_*) < 0$.
- Point E_6 corresponds to the case where the potential $V(\phi)$ is effectively constant, and thus it describes an accelerated solution dominated by the scalar field potential energy ($w_{\text{eff}} = -1$). It behaves as a saddle if $g(0) < 0$, while for $g(0) \geq 0$ one cannot use linear stability theory but center manifold theory should be employed. The analysis using this advanced tool for the case $g(0) \geq 0$ is given in appendix A.2. From that analysis, point E_6 is stable whenever $g(0) > \frac{\xi}{4}dg(0)$, while it is a saddle for $g(0) = 0$.

From the stability analysis of the critical points, depending on the choice of parameters and initial conditions, we observe that the universe starts from a stiff matter solution (points $E_{1\pm}$) and evolves either towards an accelerated, scalar field kinetic energy dominated late time attractors (points $E_{5\pm}$) or towards an accelerated, scalar field dominated late time attractor (point E_6), possibly passing through either a matter dominated solution (point E_0) or a scaling solution (point E_2). In this model, it is thus possible that the universe at late times accelerates without being driven by the scalar field potential (point $E_{5\pm}$), yet with a cosmological constant behavior ($w_{\text{eff}} = -1$). In all cases, this model can successfully describe the observed matter dominated to DE dominated transition (see Fig. 7(a) for an explicit example). We also notice the possibility of crossing the phantom divide line, as explicitly shown in Fig. 7(b) for a specific scalar field potential. This implies that in this model the scalar field characterizes a quintom scenario [61], which cannot be obtained with uncoupled

scalar (single) field models. Finally note that point E_2 represents a matter scaling solution which can again provides deviations from Λ CDM at the perturbation level, although leaving the background dynamics unchanged (see Sec. 4).

3.3.2 $\beta = 1$ case

The points $E_0, E_{1\pm}, E_2, E_3, E_4, E_{5\pm}$ found in the $\beta = 0$ case (given in table 9) are critical points of the $\beta = 1$ case as well, and their properties are unchanged. For this reason they we will not be discussed again here. The only difference is given by critical point E_6 , which now becomes a non-isolated critical set $(0, 1, z, 0)$. This set corresponds to an accelerated, scalar field dominated universe and will be denoted by E_{6z} . It is a normally hyperbolic set when $g(0) \left(1 - \frac{\xi z}{1-z}\right) \neq 0$. It is stable spiral if $4g(0) \left(1 - \frac{\xi z}{1-z}\right) > 1$, it is stable node if $0 < 4g(0) \left(1 - \frac{\xi z}{1-z}\right) < 1$, otherwise it is saddle. Note that if $1 - \frac{\xi z}{1-z} = 0$, E_{6z} reduces to point E_4 . The phenomenological aspect of the $\beta = 1$ case are the same as the $\beta = 0$ case, except that the universe can reach a de Sitter final state in a finite amount of time, namely for a non vanishing value of H (i.e. for $z \neq 0$).

4 Cosmological perturbation and structure formation

4.1 Linear perturbations and quasi-static approximation

In this section, we focus on the behavior at the perturbation level of the interacting DE models considered in the previous sections. We first present the general scalar perturbation equations at linear order, and then examine the effects arising in the process of cosmological structure formation within the quasi-static approximation.

At the background level we assume a spatially flat universe in agreement with cosmological observations, while at the linear perturbations level we work in the Newtonian gauge where the perturbed metric in Cartesian coordinates can be written as

$$ds^2 = -(1 + 2\Phi)dt^2 + (1 - 2\Psi) a^2(t) (dx^2 + dy^2 + dz^2) . \quad (4.1)$$

Since there are no anisotropic stresses in the considered coupled models [41], we take into account the equality of the scalar perturbations Φ and Ψ from the start. In other words, in what follows we will replace everywhere Φ by Ψ to simplify the equations. In the matter sector, the physical quantities to be perturbed are the matter energy density ρ , the matter pressure p , the matter four-velocity u_μ and the scalar field ϕ as

$$\rho \mapsto \rho + \delta\rho, \quad p \mapsto p + \delta p, \quad u_\mu \mapsto u_\mu + \delta u_\mu, \quad \phi \mapsto \phi + \delta\phi \quad (4.2)$$

with

$$\delta u_\mu = (-\Psi, \partial_i v) , \quad (4.3)$$

where v denotes the perturbed scalar velocity of the matter fluid. Note that the symbols ρ , p , u_μ and ϕ denote background quantities.

The derivation of the complete linear perturbed cosmological equations of Scalar-Fluid theories have been first obtained in [41, 42]. For the gradient (derivative) coupling scalar-fluid models considered in our analysis, the perturbed equations in Newtonian gauge are given by

$$\left(-\frac{k^2}{a^2} - \rho - V\right) \Psi - 3H\dot{\Psi} - \frac{1}{2}\delta\rho - \frac{1}{2}V'\delta\phi - \frac{1}{2}\dot{\phi}\delta\dot{\phi} = 0, \quad (4.4)$$

$$\dot{\Psi} + H\Psi + \frac{1}{2} \left(\rho + p - n^2 \dot{\phi} \frac{\partial f}{\partial n} \right) v - \frac{1}{2} \dot{\phi} \delta\phi = 0, \quad (4.5)$$

$$\begin{aligned} \ddot{\Psi} + 4H\dot{\Psi} + \left[3H^2 + 2\dot{H} + \frac{1}{2}\dot{\phi}^2 - \frac{1}{2}n^2\dot{\phi} \frac{\partial f}{\partial n} \right] \Psi + \frac{1}{2}\dot{\phi} \left(2\frac{\partial f}{\partial n} + n\frac{\partial^2 f}{\partial n^2} \right) \frac{n^2}{\rho+p} \delta\rho \\ - \frac{1}{2}\delta p + \frac{1}{2} \left(n^2\dot{\phi} \frac{\partial^2 f}{\partial\phi\partial n} + V' \right) \delta\phi + \frac{1}{2} \left(n^2\frac{\partial f}{\partial n} - \dot{\phi} \right) \delta\dot{\phi} = 0, \end{aligned} \quad (4.6)$$

$$\begin{aligned} 3H \left(2\frac{\partial f}{\partial n} + n\frac{\partial^2 f}{\partial n^2} \right) \frac{n^2}{\rho+p} \delta\rho + \left(2\ddot{\phi} + 6H\dot{\phi} - 3Hn^2\frac{\partial f}{\partial n} \right) \Psi + \left(4\dot{\phi} - 3n^2\frac{\partial f}{\partial n} \right) \dot{\Psi} \\ - \frac{k^2}{a^2} n^2 \frac{\partial f}{\partial n} v + \left(-\frac{k^2}{a^2} + 3Hn^2\frac{\partial^2 f}{\partial\phi\partial n} - V'' \right) \delta\phi - 3H\delta\dot{\phi} - \delta\ddot{\phi} = 0, \end{aligned} \quad (4.7)$$

$$\frac{1}{\rho+p} \left(\dot{\delta\rho} + 3H\delta p + 3H\delta\rho \right) - \frac{k^2}{a^2} v - 3\dot{\Psi} = 0, \quad (4.8)$$

$$\begin{aligned} \left(\frac{\partial\rho}{\partial n} - n\dot{\phi} \frac{\partial f}{\partial n} \right) \dot{v} + n \left[3H\dot{\phi} \left(\frac{\partial f}{\partial n} + n\frac{\partial^2 f}{\partial n^2} \right) - 3H\frac{\partial^2\rho}{\partial n^2} - \ddot{\phi} \frac{\partial f}{\partial n} - \dot{\phi}^2 \frac{\partial^2 f}{\partial\phi\partial n} \right] v + \frac{1}{n} \delta p \\ - \dot{\phi} \left(2\frac{\partial f}{\partial n} + n\frac{\partial^2 f}{\partial n^2} \right) \frac{n}{\rho+p} \delta\rho + \frac{\partial\rho}{\partial n} \Psi - n \left(3H\frac{\partial f}{\partial n} + \dot{\phi} \frac{\partial^2 f}{\partial\phi\partial n} \right) \delta\phi - n\frac{\partial f}{\partial n} \delta\dot{\phi} = 0. \end{aligned} \quad (4.9)$$

We will analyze the implications of the perturbation equations (4.4)-(4.9) on structure formation when the quasi-static approximation is considered. The scope is to investigate the evolution of matter overdensities δ (where δ is given by $\frac{\delta\rho}{\rho}$) in the comoving matter gauge. In order to simplify the following equations, we introduce the background quantities [41]:

$$X = n^2 \frac{\partial^2 f}{\partial\phi\partial n}, \quad Y = n^2 \frac{\partial f}{\partial n}, \quad Z = n^3 \frac{\partial^2 f}{\partial n^2}. \quad (4.10)$$

Moreover from now on we assume cold DM ($w = 0$), with energy density proportional to the fluid particle number density n (namely $\rho \propto n$). This implies that the sound speed square of the fluid in the rest frame of the field

$$c_s^2 \equiv n \frac{\rho_{,nn}}{\rho_{,n}}, \quad (4.11)$$

vanishes. The evolution equation for matter overdensities in the comoving matter gauge is then given by [41]

$$\ddot{\delta} + \left[2H + \frac{V'Y + Y'(2Y - \dot{\phi})\dot{\phi}}{\rho + Y(Y - \dot{\phi})} \right] \dot{\delta} = \frac{\rho}{2} \left[1 + \frac{Y(Y - \dot{\phi})}{\rho} \right]^{-1} \delta, \quad (4.12)$$

where a prime denotes differentiation with respect to ϕ .

In what follows we are going to explore how Eq. (4.12) behaves in the standard matter dominated and scaling solutions obtained for both models I and II in Sec. 3. These solutions can in fact be used to consistently describe the structure formation era of the universe at

the background level, but deviations from the standard Λ CDM dynamics might appear at the perturbations level. Note that for all these solutions, being them critical points where $w_{\text{eff}} = w = 0$, the Hubble parameter scales as

$$H = \frac{2}{3(1 + w_{\text{eff}})(t - t_0)} = \frac{2}{3(t - t_0)}, \quad (4.13)$$

where t_0 is a constant of integration which we set to be 0 for simplicity. This is indeed the expected background evolution in a matter dominated universe.

4.2 Model I

The background quantities (4.10) can always be rewritten in terms of the dimensionless variables (3.1). Specifically for Model I they can be expressed as

$$X = -\gamma H \sigma^{1-2\alpha} y^{2\alpha} \left(\alpha s^{\beta+1} + \beta s^{\beta-1} g(s) \right), \quad (4.14)$$

$$Y = -\xi H s^\beta y^{2\alpha} \sigma^{1-2\alpha}, \quad (4.15)$$

$$Z = 2\xi H s^\beta y^{2\alpha} \sigma^{1-2\alpha}. \quad (4.16)$$

Note that now one can directly relate the growth rate evolution equation (4.12) with the coordinates of the critical points obtained from the background analysis in Sec. 3.

4.2.1 (0,0) model

According to Sec. 3.2.1, for this model we have only one critical point corresponding to a matter scaling solution, namely point A_3 (we will ignore the special case $s_*^2 = 3$ where also A_2 describes a matter scaling solution). For this point, Eq. (4.12) reduces to

$$\ddot{\delta} + \frac{4}{3t} \dot{\delta} = \frac{2}{t^2 (2\xi^2 + 3)} \delta. \quad (4.17)$$

This equation can also be written as

$$\delta'' + \frac{1}{2} \delta' = \frac{9}{2 (2\xi^2 + 3)} \delta \quad (4.18)$$

where prime denotes derivative with respect to N , by using the relation $\frac{d}{dN} = \frac{1}{H} \frac{d}{dt}$. The general solution of Eq. (4.18) is given by

$$\delta = C_1 a^{m_+} + C_2 a^{m_-}, \quad (4.19)$$

where C_1 and C_2 are two constant of integration, and

$$m_+ = \frac{(-3 - 2\xi^2 + \sqrt{225 + 156\xi^2 + 4\xi^4})}{4(3 + 2\xi^2)}, \quad m_- = \frac{(-3 - 2\xi^2 - \sqrt{225 + 156\xi^2 + 4\xi^4})}{4(3 + 2\xi^2)}. \quad (4.20)$$

We can notice that in this case the growth rate of matter perturbations depends only on the parameter ξ . Moreover the quantity m_- is always negative, and thus it does not contribute to the growth of perturbations. For m_+ we have $0 \leq m_+ \leq 1$, which implies that the growth rate for this interacting DE model is smaller than that of the uncoupled case where $\delta \propto a$ [12], which is correctly recovered for $\xi = 0$.

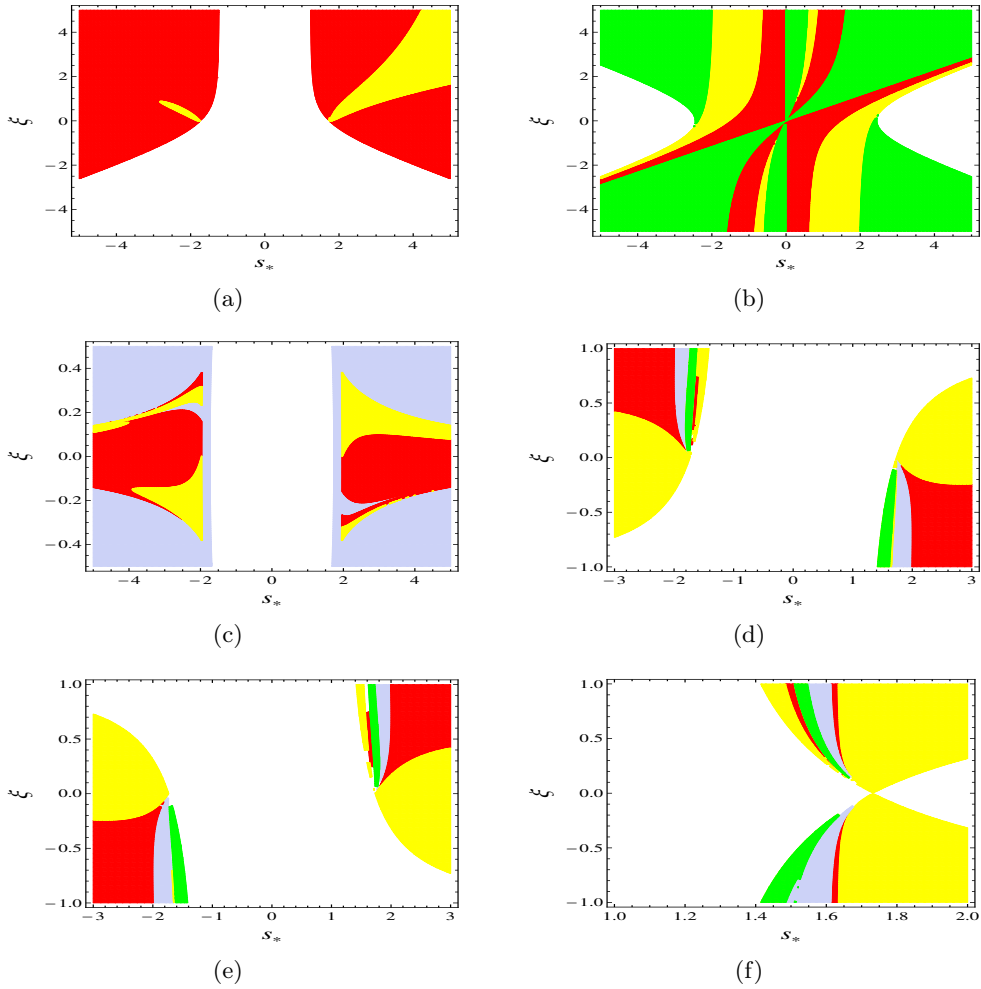


Figure 8: The red regions in the (s_*, ξ) parameter space denote the areas where $m_+ > 1$, the yellow regions denote the areas where $m_+ < 1$, the blue regions denote the areas where m_+ is imaginary (i.e. matter perturbations are oscillating) and the green regions denote the areas where $m_+ < 0$. Panels (a) and (b) correspond respectively to points B_8 and B_9 of the $(0, \frac{1}{2})$ model. Panel (c) corresponds to point C_3 of the $(1, 0)$ model. Panels (d), (e) and (f) correspond respectively to points D_{2+} , D_{2-} and D_4 of the $(1, \frac{1}{2})$ model.

4.2.2 $(0, \frac{1}{2})$ model

This model coincides with the k -essence scalar field model studied in [47, 60] at the background level. For this model, we obtain one standard matter dominated critical point B_1 , one matter scaling solution B_8 and one scaling solution B_9 (see [47]). For point B_1 the quantities X , Y , Z vanish, hence Eq. (4.12) reduces to that derived within the Λ CDM model, implying that there are no deviations from Λ CDM dynamics even at perturbation level. For point B_8 , the growth rate depends on the parameters s_* and ξ , and the perturbation equation (4.12)

becomes

$$\begin{aligned} \ddot{\delta} + \frac{1}{3} \frac{(\xi + \eta) \xi (6 s_* \xi - 2 \xi^2 + \sqrt{3}) - 12(\eta \xi + 2) + 2(s_* - \xi) (4 s_* + 7 \xi)}{t ((\xi^3 + \sqrt{3} \xi) (\xi + \eta) - 3(\eta \xi + 2) + 2(s_*^2 - \xi^2))} \dot{\delta} \\ = \frac{1}{3} \frac{(3 \eta (\xi + \eta) - 2 s_*^2)^2}{s_*^2 t^2 (3 \sqrt{3} \xi (\xi + \eta) (\xi^2 + \sqrt{3}) - 3(\eta \xi + 2) + 2 s_*^2)} \delta, \end{aligned} \quad (4.21)$$

where $\eta = \sqrt{\xi^2 + 2}$. The solution of this equation has the same form as (4.19), with m_+ and m_- depending only on s_* and ξ . We will not report here the relation of m_{\pm} with s_* and ξ due to their complicated and long expressions. Nevertheless in Fig. 8(a) we have plotted the regions where the quantity $m_+ > 1$, i.e. when the growth rate is enhanced by the coupling in comparison to that of uncoupled models, the regions where $m_+ < 1$, i.e. when the growth rate is slower in comparison to that of uncoupled models. We have checked that m_+ is not imaginary and that $m_- < 1$ for any values of s_* and ξ . Finally for point B_9 we recover an equation similar to Eq. (4.21), which however will not be shown due to the long expressions of its coefficients. We can however mention that the quantity m_+ depends on both s_* and ξ , while m_- vanishes. Also for this case, we have plotted in Fig. 8(b) the regions where the quantity $m_+ > 1$, the regions where $m_+ < 1$ and also the regions where $m_+ < 0$.

4.2.3 (1, 0) model

According to Sec. 3.2.2, for this model we have one standard matter dominated critical point C_0 , one matter scaling solution C_2 and one scaling solution C_3 . For point C_0 the quantities X, Y, Z vanish again, meaning that Eq. (4.12) reduces to that obtained within the Λ CDM model. For point C_2 Eq. (4.12) reduces instead to

$$\ddot{\delta} + \frac{4}{3t} \dot{\delta} = \frac{2}{3} \frac{2 s_*^2 \xi^2 + 1}{t^2 (2 s_*^2 \xi^2 + 3)} \delta \quad (4.22)$$

We obtain again the general solution as

$$\delta = C_1 a^{m_+} + C_2 a^{m_-}, \quad (4.23)$$

where now

$$m_{\pm} = \frac{(-3 - 2 s_*^2 \xi^2 \pm \sqrt{81 + 204 s_*^2 \xi^2 + 100 s_*^4 \xi^4})}{4(3 + 2 s_*^2 \xi^2)}. \quad (4.24)$$

Note that in this case the growth rate of matter perturbations depends only on the combination $s_*^2 \xi^2$. Moreover we find again $m_- < 0$ and $0 \leq m_+ \leq 1$, which implies that the growth rate for this case is always smaller than that of uncoupled models. Finally for point C_3 Eq. (4.12) becomes

$$\begin{aligned} \ddot{\delta} - \frac{2}{3t} \frac{s_*^2 (-3 \xi s_* \sqrt{-2 \Omega} (\Delta \sqrt{2} s_* - 4) + 4 s_*^2 \xi^2 + 12)}{\Theta (s_*^2 \xi^2 \Omega - 3 \xi s_* \sqrt{-2 \Omega} + 3 \Omega)} \dot{\delta} \\ = -\frac{8}{3t^2} \frac{s_* \Omega \sqrt{-2 \Omega}}{\Theta^2 \left(\sqrt{-2 \Omega} s_* \xi^2 + \frac{\sqrt{-2 \Omega}}{s_*} + 6 \xi \right)} \delta, \end{aligned} \quad (4.25)$$

where

$$\Theta = \left(-\xi \sqrt{2 s_*^2 \xi^2 + 4 s_*^2 - 2 \Delta - 12 s_*} - s_*^2 \xi^2 - 2 s_*^2 + \Delta \right), \quad (4.26)$$

$$\Delta = \sqrt{\xi^2 s_*^2 ((\xi^2 + 4) s_*^2 - 12)}, \quad (4.27)$$

$$\Omega = \Delta^2 - 2 s_*^2 + 3. \quad (4.28)$$

The growth rate results in a complicated expression depending on the parameters s_* and ξ , however we have checked that $m_- < 0$ for any s_* and ξ . In order to understand the behavior of the growth rate for some values of these parameters, in Fig. 8(c) we have numerically plotted the regions in the (s_*, ξ) parameter space where the exponent m_+ is greater or smaller than 1. This gives the regions in which matter overdensities grow faster or slower than in the uncoupled case.

4.2.4 $(1, \frac{1}{2})$ model

According to Sec. 3.2.3, for this model we obtain one standard matter dominated critical point D_0 , two matter scaling solutions $D_{2\pm}$ and one general scaling solution D_4 . As expected for point D_0 the quantities X, Y, Z vanish, implying that there are no deviations from standard Λ CDM dynamics even at the perturbations level. For point D_{2+} , Eq. (4.12) becomes

$$\begin{aligned} \ddot{\delta} - \frac{1}{3} \frac{(\xi s_* + \Delta) s_* \xi (2 s_*^2 \xi^2 - 6 s_*^2 \xi + 9) + 6 s_*^2 (\xi - 4) (\xi + 1) + 72}{t (s_*^3 \xi^3 (\xi s_* + \Delta) + 3 s_*^2 \xi^2 + 6 s_*^2 - 18)} \dot{\delta} \\ = \frac{1}{3} \frac{(\Delta s_* \xi + \Delta^2 - 2 s_*^2)^2}{s_*^2 t^2 (s_*^4 \xi^4 + \Delta s_*^3 \xi^3 + 2 \Delta s_* \xi + 5 \Delta^2 + 2 s_*^2 - 36)} \delta, \end{aligned} \quad (4.29)$$

where $\Delta = \sqrt{\xi^2 s_*^2 + 6}$. As in the previous cases, we have plotted in Fig. 8(d) the regions on the (s_*, ξ) parameter space where $m_+ > 1$, $m_+ < 1$, $m_+ < 0$ and where m_+ is imaginary. We have also checked that either $m_- < 1$ or imaginary. A similar plot for point D_{2-} is provided in Fig. 8(e) (we do not present explicitly the equivalent to Eq. (4.12) for point D_{2-}), and again we either find $m_- < 1$ or imaginary for every choice of the parameters. Finally for point D_4 Eq. (4.12) becomes

$$\begin{aligned} \ddot{\delta} - \frac{4 s_*^4 (s_*^2 \xi (2 s_*^4 \xi - 6 s_*^4 - 15 s_*^2 \xi + 36 s_*^2 + 63 \xi - 54) - 6 \Theta)}{3 t (2 s_*^6 \xi^2 - 6 s_*^4 \xi^2 + 3 \Theta)} \dot{\delta} \\ = \frac{4 s_*^4 \Theta^2}{3 t^2 \xi^2 (2 s_*^4 + 9 s_*^2 - 18)^2 (2 s_*^6 \xi^2 - 2 s_*^4 \xi^2 + \Theta)} \delta, \end{aligned} \quad (4.30)$$

where $\Theta = (2 s_*^4 \xi^2 - 2 s_*^4 - 3 s_*^2 \xi^2 + 12 s_*^2 - 18)$. For this case we have plotted as well in Fig. 8(f) the regions in the (s_*, ξ) parameter space where $m_+ > 1$ (regions where matter overdensities grow faster than the uncoupled case), $m_+ < 1$ (regions where matter overdensities grow slower than the uncoupled case), $m_+ < 0$ and where m_+ is imaginary. We have also checked numerically that m_- is either < 1 or imaginary for any values of s_* and ξ .

4.3 Model II

From Eqs. (4.10) we find that for Model II X vanishes, while $Y = -\xi H_0$ and $Z = 2 \xi H_0$. In both $\beta = 0$ and $\beta = 1$ cases, we obtain one standard matter dominated critical point E_0 and one matter scaling solution E_2 (cf. Sec. 3.3). Since point E_0 is independent of the potential

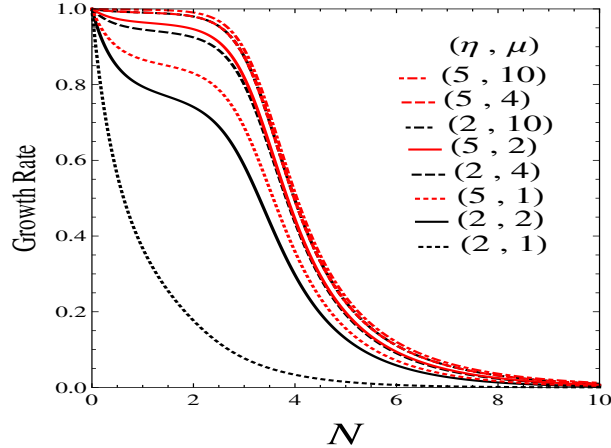


Figure 9: Plot of the growth rate $\frac{d \ln \delta}{dN}$ versus N for Model II with $\beta = 0$ and the scalar field potential $V = V_0 \sinh^{-\eta}(\mu\phi)$ with $\xi = 1$ and $V_0 = H_0^2$.

for its existence, its behavior at the perturbation level is the same as that derived in the case of an exponential potential. This case has already been analysed in [41], and thus will not be considered here. Point E_2 instead depends on the choice of the scalar field potentials, and thus its dynamics at the perturbation level will be different for different potentials. In what follows we present an explicit example choosing the scalar field potential as

$$V(\phi) = V_0 \sinh^{-\eta}(\mu\phi), \quad (4.31)$$

where V_0 , η and μ are parameters of suitable dimension. For this potential we find $s_* = \pm\mu\eta$ and Eq. (4.12) yields

$$\ddot{\delta} + \left[2H + \frac{3}{2} \frac{\eta \mu \xi^2 H_0 \sqrt{1 + \left(\frac{9H^2}{2s_*^2 V_0} \right)^{\frac{2}{\eta}}}}{H_0^2 s_*^2 \xi^2 + 3H^2 s_*^2 + 3HH_0 s_* \xi - 9H^2} \right] \dot{\delta} = \frac{9}{2s_*^2} \frac{(s_*^2 - 3)^2 H^4}{(H_0^2 s_*^2 \xi^2 + 3H^2 s_*^2 + 3H_0 s_* \xi - 9H^2)} \delta. \quad (4.32)$$

Note that the general solution of this equation is not of the form provided in Eq. (4.19), since the coefficients now are no longer constant being H generally time dependent (cf. Eq. (4.13)). We solve this equation numerically and present the evolution of the growth rate in Fig. 9. From this figure, we notice that at higher redshift (small N) and for sufficiently high values of η and μ , the matter overdensities grow at a constant rate, similar to the Λ CDM result where $d \ln \delta / dN = 1$ always. For lower values of the parameters instead we find a growth rate which differs from the standard Λ CDM results even at early times. Furthermore we have checked that for $\beta = 0$ if $\eta < 0$ and $\mu > 0$ the growth rate becomes $\gg 1$ and grows indefinitely as N increases. This reduces the region in (η, μ) parameter space which can give an evolution of matter perturbation comparable to the observed behavior of the universe. A similar plot can be obtained for the $\beta = 1$ choice, but in this case the growth rate is $\gg 1$ and grows indefinitely as N increases when $\eta > 0$ and $\mu < 0$.

5 Conclusion

In this paper we investigated the cosmological evolution of scalar field DE models with gradient coupling to the DM fluid, i.e. where a coupling between the derivative of the scalar field $\partial_\mu\phi$ and the fluid's 4-velocity u_μ is present. This coupling has been realised at the Lagrangian level by considering the consistent variational approach introduced in [39]. The coupling term appearing in the Lagrangian has the general expression given by $\sqrt{-g}f(\mathbf{n}, \mathbf{s}, \phi)/\mathbf{n}(u^\mu\partial_\mu\phi)$, where f is an arbitrary function of all its arguments. Generalising the analysis of [39], we have considered two models corresponding to two distinct choices of the coupling function $f(\mathbf{n}, \mathbf{s}, \phi)$ (see Table 1).

The first objective of the present paper was to investigate the background dynamics of these interacting DE models for arbitrary self interacting potentials. For this analysis we have employed well-known dynamical systems methods, which allowed us to explore the complete cosmological evolution of the models considered. In general we found that different interesting cosmological solutions can be obtained (see Sec. 3) from these models: the observed late-time transition from matter domination to DE domination, matter scaling solutions, late-time accelerating scaling solutions (useful to solve the cosmic coincidence problem) and even possible crossing of the phantom barrier. This implies that these interacting models can produce interesting phenomenology at cosmological distances, able to reproduce the observed evolution of the universe, and possible deviations from it, at the background level.

Moreover for each of the models analysed we found matter scaling solutions able to successfully describe the matter dominated era at the background level, but possibly giving deviations in the dynamics of linear perturbations. For this reason the second objective of our investigation was to analyse the cosmological dynamics at the perturbation level. In particular we studied the formation of cosmological structures within the quasi-static approximation (see Sec. 4). All the scaling solutions found in the background analysis of Sec. 3 present deviations from the standard Λ CDM dynamics during the growth of cosmological structure. We have parametrized and discussed these deviations in Sec. 4, and provided explicit examples to better understand the differences with the standard cosmological scenario. These deviations can in principle be constrained by observational data, providing in turn constraints on the free parameters characterizing the interaction of DE with DM in these models. The confrontation with observational data is however outside the scope of the present analysis and will be left as material for future work.

In conclusion we studied here the cosmological dynamics, at both background and perturbation levels, of interacting DE models where a gradient coupling between a scalar field and a matter fluid has been implemented using the variational approach introduced in [39]. These DE models expand the possible theoretical arena where an interaction in the dark sector can be well defined at the fully covariant level, providing in this way consistent equations of motion at both background and perturbations cosmological levels. The dynamics obtained from these equations can thus be effectively used to find deviations from the standard Λ CDM evolution which can eventually be tested against the observations, and thus used to constrain the parameter space of these interacting DE models.

Acknowledgments

J.D. is thankful to IUCAA for warm hospitality and its facility for doing research work. N.T. acknowledges support from the Labex P2IO and an Enhanced Eurotalents Fellowship.

A Appendix: Center Manifold Theory (CMT)

A.1 General framework

Without going into the mathematical background of center manifold theory, in the following we list some important steps on determining the dynamics of a center manifold near a critical point. For more mathematical details and examples, we refer the reader to [56, 57].

If the non-vanishing eigenvalues of the Jacobian matrix of a non-hyperbolic critical points have all negative real part (if at least one of them has positive real part then the point is unstable), then the stability of the critical point can be determined using CMT with the following operational steps:

1. First translate the coordinates of the non-hyperbolic critical point under consideration to the origin and obtain a new set of autonomous equations in the new coordinates.
2. Express the non linear autonomous system of equations obtained in step 1 into the following standard form

$$u' = Au + f(u, v) \tag{A.1}$$

$$v' = Bv + g(u, v) \tag{A.2}$$

where $(u, v) \in \mathbb{R}^c \times \mathbb{R}^s$ with f and g satisfying

$$f(0, 0) = 0, \quad Df(0, 0) = 0$$

$$g(0, 0) = 0, \quad Dg(0, 0) = 0$$

Here A is a $c \times c$ matrix whose eigenvalues have zero real part, B is $s \times s$ matrix whose eigenvalues have negative real part and Df denotes the Jacobian matrix of f .

3. Determine a function $h(u)$, usually approximating it by a series expansion, which is at least C^2 and satisfies the following quasilinear partial differential equation

$$\mathcal{N}h(u) \equiv Dh(u) (Au + f(u, h(u)) - Bh(u) - g(u, h(u))) = 0, \tag{A.3}$$

with $h(0) = 0$ and $Dh(0) = 0$.

4. The dynamics of the original system restricted to the center manifold is then determined by substituting the approximated solution of h obtained in step 3 in the equation

$$u' = Au + f(u, h(u)) \tag{A.4}$$

The stability/instability of the system (A.4) implies the stability/instability of the original system. Note that usually Eq. (A.4) reads $u' = ku^n$ for some constant k and positive integer number n (the lowest order in the expansion), for which stability is achieved only if $k < 0$ and n is odd-parity, while any other case yield instability [57].

In what follows we explicitly show some examples of this analysis that have been used in the main body of the paper. This should help the reader to better understand the practical application of the steps outlined above.

A.2 Applications of CMT

Center manifold dynamics for point C_5 of model I with $\beta = 1$, $\alpha = 0$ when $g(0) = 0$

In this appendix we apply CMT to study the stability of point C_5 appearing in the analysis of Sec. 3.2.2. The coordinates of this point are $(x, y, s) = (0, 1, 0)$ (cf. Table 5). We first translate the point $(0, 1, 0)$ to the origin by using the transformation $x \rightarrow x$, $y \rightarrow y + 1$, $s \rightarrow s$. Then Eqs. (3.5)-(3.7) becomes

$$x' = -\frac{1}{2} \left(3x((w-1)x^2 + (w+1)(y+1)^2 + 1 - w) - \sqrt{6}(\xi \sqrt{1-x^2 - (y+1)^2} s(x^2 - 1) + s(y+1)^2) \right), \quad (\text{A.5})$$

$$y' = -\frac{1}{2}(y+1) \left(3((w-1)x^2 + (w+1)((y+1)^2 - 1)) + \sqrt{6}x(s - \xi \sqrt{1-x^2 - (y+1)^2} s) \right), \quad (\text{A.6})$$

$$s' = -\sqrt{6} x g(s). \quad (\text{A.7})$$

Using the eigenvectors of the Jacobian matrix of the transformed system, we now introduce a new set of variables defined by

$$\begin{pmatrix} X \\ Y \\ S \end{pmatrix} = \begin{pmatrix} 1 & 0 & -\frac{1}{\sqrt{6}} \\ 0 & 1 & 0 \\ 0 & 0 & 1 \end{pmatrix} \begin{pmatrix} x \\ y \\ s \end{pmatrix}$$

In terms of these new set of variables, the system of equations can now be written as

$$\begin{pmatrix} X' \\ Y' \\ S' \end{pmatrix} = \begin{pmatrix} -3 & 0 & 0 \\ 0 & -3(w+1) & 0 \\ 0 & 0 & 0 \end{pmatrix} \begin{pmatrix} X \\ Y \\ S \end{pmatrix} + \begin{pmatrix} g_1 \\ g_2 \\ f \end{pmatrix}$$

where f , g_1 , g_2 are polynomials of degree greater than 2 in (X, Y, S) with

$$f(X, Y, S) = -\sqrt{6}g(S)X - g(S)S \quad (\text{A.8})$$

whereas g_1 , g_2 are not shown due to their lengths. Now, the coordinates which correspond to non-zero eigenvalues (X, Y) can be approximated in terms of S by the expanded functions

$$h_1(S) = a_2 S^2 + a_3 S^3 + \mathcal{O}(S^4), \quad (\text{A.9})$$

$$h_2(S) = b_2 S^2 + b_3 S^3 + \mathcal{O}(S^4), \quad (\text{A.10})$$

respectively. The quasilinear partial differential equation which the function vector

$$\mathbf{h} = \begin{pmatrix} h_1 \\ h_2 \end{pmatrix},$$

has to satisfy, is given by

$$D\mathbf{h}(\mathbf{S}) [AS + \mathbf{F}(S, \mathbf{h}(S))] - B\mathbf{h}(S) - \mathbf{g}(S, \mathbf{h}(S)) = \mathbf{0}, \quad (\text{A.11})$$

with

$$\mathbf{g} = \begin{pmatrix} g_1 \\ g_2 \end{pmatrix}, \quad \mathbf{F} = f, \quad B = \begin{pmatrix} -3 & 0 \\ 0 & -3(w+1) \end{pmatrix}, \quad A = 0.$$

In order to solve the Eq. (A.11), we substitute $A, \mathbf{h}, \mathbf{F}, B, \mathbf{g}$ into it and equate equal powers of S in order to obtain $\mathbf{h}(S)$ up to the desired order. By comparing powers of S from both sides of Eq. (A.11) we obtain the constants a_2, a_3, b_2, b_3 as

$$a_2 = -\frac{\sqrt{6}}{18}dg(0), \quad a_3 = \frac{\sqrt{6}}{36}(2dg(0)^2 + d^2g(0)), \quad b_2 = -\frac{1}{12}, \quad b_3 = -\frac{1}{18}dg(0). \quad (\text{A.12})$$

Finally the dynamics of the reduced system is determined by the equation

$$S' = AS + \mathbf{F}(S, \mathbf{h}(S)), \quad (\text{A.13})$$

so that

$$S' = -dg(0)S^2 - \left(\frac{1}{3}dg(0) + \frac{1}{2}d^2g(0) \right) S^3 + \mathcal{O}(S^4). \quad (\text{A.14})$$

Hence point C_5 is always unstable since at the lowest order we obtain an even-parity term. If instead $dg(0) = 0$ then the next term in the expansion must be considered, in which case the point is stable if $d^2g(0) > 0$.

Center manifold dynamics for point $D_{5\pm}$ of model I with $\beta = 1, \alpha = \frac{1}{2}$ when $g(0) = 0$

In this appendix we apply center manifold theory to study the stability of point D_{5+} with coordinates $(x, y, s) = (0, 1, 0)$ and D_{5-} with coordinates $(0, -1, 0)$ for the cases where $g(0) = 0$ (see Sec. 3.2.3). We first analyze point D_{5+} . We translate the point $(0, 1, 0)$ to the origin by using the transformation $x \rightarrow x, y \rightarrow y + 1, s \rightarrow s$. Then Eqs. (3.5)-(3.7) becomes

$$x' = -\frac{1}{2} \left(3x((w-1)x^2 + (w+1)(y+1)^2 + 1 - w) - \sqrt{6}(\xi(y+1)s(x^2 - 1) + s(y+1)^2) \right), \quad (\text{A.15})$$

$$y' = -\frac{1}{2}(y+1) \left(3((w-1)x^2 + (w+1)((y+1)^2 - 1)) + \sqrt{6}x(s - \xi(y+1)s) \right), \quad (\text{A.16})$$

$$s' = -\sqrt{6}xg(s). \quad (\text{A.17})$$

Using the eigenvectors of the stability matrix of the transformed system, we now introduce a new set of variables given by

$$\begin{pmatrix} X \\ Y \\ S \end{pmatrix} = \begin{pmatrix} 0 & 1 & 0 \\ 1 & 0 & \frac{(\xi-1)}{\sqrt{6}} \\ 0 & 0 & 1 \end{pmatrix} \begin{pmatrix} x \\ y \\ s \end{pmatrix}$$

In terms of these new set of variables, the system of equations (A.17)-(A.17) can now be written as

$$\begin{pmatrix} X' \\ Y' \\ S' \end{pmatrix} = \begin{pmatrix} -3(w+1) & 0 & 0 \\ 0 & -3 & 0 \\ 0 & 0 & 0 \end{pmatrix} \begin{pmatrix} X \\ Y \\ S \end{pmatrix} + \begin{pmatrix} g_1 \\ g_2 \\ f \end{pmatrix}$$

where f, g_1, g_2 are polynomials of degree greater than 2 in (X, Y, S) with

$$f(X, Y, Z, S) = -\sqrt{6}g(S)Y + g(S)\xi S - g(S)S \quad (\text{A.18})$$

whereas g_1, g_2 are not shown due to their lengths. Now the coordinates which correspond to non-zero eigenvalues (X, Y) can be approximated in terms of S by the functions

$$h_1(S) = a_2 S^2 + a_3 S^3 + \mathcal{O}(S^4), \quad (\text{A.19})$$

$$h_2(S) = b_2 S^2 + b_3 S^3 + \mathcal{O}(S^4), \quad (\text{A.20})$$

respectively. The quasilinear partial differential equation which the vector of functions

$$\mathbf{h} = \begin{pmatrix} h_1 \\ h_2 \end{pmatrix}$$

has to satisfy, is given by

$$D\mathbf{h}(\mathbf{S}) [AS + \mathbf{F}(S, \mathbf{h}(S))] - B\mathbf{h}(S) - \mathbf{g}(S, \mathbf{h}(S)) = \mathbf{0}, \quad (\text{A.21})$$

where

$$\mathbf{g} = \begin{pmatrix} g_1 \\ g_2 \end{pmatrix}, \quad \mathbf{F} = f, \quad B = \begin{pmatrix} -3(w+1) & 0 \\ 0 & -3 \end{pmatrix}, \quad A = 0.$$

In order to solve the Eq. (A.21), we substitute $A, \mathbf{h}, \mathbf{F}, B, \mathbf{g}$ in it and equate equal powers of S in order to obtain $\mathbf{h}(S)$ up to the desired order. This process yields the values of the constants a_2, a_3, b_2, b_3 as

$$\begin{aligned} a_2 &= -\frac{1}{12}(\xi - 1)^2, & a_3 &= \frac{1}{18}(\xi - 1)^3 dg(0), & b_2 &= \frac{\sqrt{6}}{18}(\xi - 1)^2 dg(0), \\ b_3 &= -\frac{\sqrt{6}}{72}(\xi - 1)^2 (4dg(0)^2(1 - \xi) + 2d^2g(0) + \xi) \end{aligned} \quad (\text{A.22})$$

Now the dynamics of the reduced system is determined by the equation

$$S' = AS + \mathbf{F}(S, \mathbf{h}(S)), \quad (\text{A.23})$$

which becomes

$$S' = -dg(0)(1 - \xi)S^2 + \frac{1}{6}(\xi - 1) (2dg(0)^2(1 - \xi) + 3d^2g(0)) S^3 + \mathcal{O}(S^4). \quad (\text{A.24})$$

This implies that point D_{5+} is always unstable, unless either $dg(0) = 0$ or $\xi = 1$. If $dg(0) = 0$ then the point is stable if $d^2g(0)(1 - \xi) > 0$, if instead $\xi = 1$ higher order terms in the expansion must be considered in order to determine stability. A similar analysis can be performed for point D_{5-} , eventually leading to the equation

$$S' = -dg(0)(1 + \xi)S^2 - \frac{1}{6}(\xi + 1) (2dg(0)^2(1 + \xi) + 3d^2g(0)) S^3 + \mathcal{O}(S^4). \quad (\text{A.25})$$

Consequently, the point D_{5-} is unstable unless either $dg(0) = 0$ or $\xi = -1$, in which cases higher order terms must be analysed to determine its stability.

Center manifold dynamics for point E_6 of model II when $g(0) > 0$

In this appendix we apply center manifold theory to study the stability of point E_6 of Model II with coordinates $(x, y, z, s) = (0, 1, 0, 0)$ when $g(0) > 0$ (see Sec. 3.3.1). First we translate the point $(0, 1, 0, 0)$ to the origin by using the transformation $x \rightarrow x$, $y \rightarrow y + 1$, $z \rightarrow z$, $s \rightarrow s$. Then Eqs. (3.17)-(3.20) become

$$x' = -\frac{1}{2(z-1)} \left[3x(z-1)(1-w+(w-1)x^2+(1+w)(y+1)^2) + \sqrt{6}(-\xi z(1-x^2)-s(z-1)(y+1)^2) \right], \quad (\text{A.26})$$

$$y' = -\frac{(y+1)}{2(z-1)} \left[3(z-1)((1+w)((y+1)^2-1)+(w-1)x^2) + \sqrt{6}x((z-1)s+z\xi) \right], \quad (\text{A.27})$$

$$z' = \frac{z}{2} \left[3(z-1)((1+w)((y+1)^2-1)+(w-1)x^2) + \sqrt{6}z\xi x \right], \quad (\text{A.28})$$

$$s' = -\sqrt{6}xg(s). \quad (\text{A.29})$$

Using the eigenvectors of the stability matrix of the transformed system, we now introduce a new set of variables given by

$$\begin{pmatrix} X \\ Y \\ Z \\ S \end{pmatrix} = \begin{pmatrix} 0 & 1 & 0 & 0 \\ -\frac{\sqrt{6}g(0)}{\sqrt{9+12g(0)}} & 0 & \frac{1}{2} \frac{\xi(3+\sqrt{9+12g(0)})}{\sqrt{9+12g(0)}} & \frac{1}{2} \frac{(3+\sqrt{9+12g(0)})}{\sqrt{9+12g(0)}} \\ \frac{\sqrt{6}g(0)}{\sqrt{9+12g(0)}} & 0 & \frac{1}{2} \frac{\xi(-3+\sqrt{9+12g(0)})}{\sqrt{9+12g(0)}} & \frac{1}{2} \frac{(-3+\sqrt{9+12g(0)})}{\sqrt{9+12g(0)}} \\ 0 & 0 & \xi & 0 \end{pmatrix} \begin{pmatrix} x \\ y \\ z \\ s \end{pmatrix}$$

In terms of these new set of variables, the system of equations can now be written as

$$\begin{pmatrix} X' \\ Y' \\ Z' \\ S' \end{pmatrix} = \begin{pmatrix} -3(w+1) & 0 & 0 & 0 \\ 0 & \frac{3}{2} \frac{4g(0)-\sqrt{9+12g(0)}+3}{\sqrt{9+12g(0)}} & 0 & 0 \\ 0 & 0 & -\frac{3}{2} \frac{\sqrt{9+12g(0)}+4g(0)+3}{\sqrt{9+12g(0)}} & 0 \\ 0 & 0 & 0 & 0 \end{pmatrix} \begin{pmatrix} X \\ Y \\ Z \\ S \end{pmatrix} + \begin{pmatrix} g_1 \\ g_2 \\ g_3 \\ f \end{pmatrix}$$

where f, g_1, g_2, g_3 are polynomials of degree greater than 2 in (X, Y, Z, S) which will not be written down due to their length. At this point the coordinates which correspond to non-zero eigenvalues (X, Y, Z) can be approximated in terms of S by the expanded functions

$$h_1(S) = a_2 S^2 + a_3 S^3 + \mathcal{O}(S^4), \quad (\text{A.30})$$

$$h_2(S) = b_2 S^2 + b_3 S^3 + \mathcal{O}(S^4), \quad (\text{A.31})$$

$$h_3(S) = c_2 S^2 + c_3 S^3 + \mathcal{O}(S^4), \quad (\text{A.32})$$

respectively. The vector composed by these functions, namely

$$\mathbf{h} = \begin{pmatrix} h_1 \\ h_2 \\ h_3 \end{pmatrix}$$

has to satisfy the following differential equation

$$D\mathbf{h}(\mathbf{S}) [AS + \mathbf{F}(S, \mathbf{h}(S))] - B\mathbf{h}(S) - \mathbf{g}(S, \mathbf{h}(S)) = \mathbf{0}. \quad (\text{A.33})$$

with

$$\mathbf{g} = \begin{pmatrix} g_1 \\ g_2 \\ g_3 \end{pmatrix}, \quad \mathbf{F} = f, \quad A = 0, \quad B = \begin{pmatrix} -3(w+1) & 0 & 0 \\ 0 & \frac{3}{2} \frac{4g(0) - \sqrt{9+12g(0)} + 3}{\sqrt{9+12g(0)}} & 0 \\ 0 & 0 & -\frac{3}{2} \frac{\sqrt{9+12g(0)} + 4g(0) + 3}{\sqrt{9+12g(0)}} \end{pmatrix}. \quad (\text{A.34})$$

Finally in order to solve Eq. (A.33), we substitute A , \mathbf{h} , \mathbf{F} , B , \mathbf{g} into it and equate equal powers of S to obtain $\mathbf{h}(S)$ order by order. On comparing powers of S from both sides of Eq. (A.33) we obtain the constants $a_2, a_3, b_2, b_3, c_2, c_3$ as

$$a_2 = 0, \quad a_3 = 0, \quad b_2 = \frac{4g(0) + \sqrt{9+12g(0)} + 3}{2\xi(4g(0) + 3)}, \quad c_2 = -\frac{\sqrt{9+12g(0)} - 4g(0) - 3}{2\xi(4g(0) + 3)},$$

$$b_3 = -\frac{1}{2g(0)(4g(0) + 3)^2 \xi^2} \left[8dg(0)\xi(g(0))^2 + 4(g(0))^2 \sqrt{9+12g(0)} \right. \\ \left. + 3dg(0)\xi \sqrt{9+12g(0)} - 16(g(0))^3 + 18dg(0)\xi g(0) \right. \\ \left. - 9\sqrt{9+12g(0)}g(0) - 48(g(0))^2 + 9dg(0)\xi - 27g(0) \right],$$

$$c_3 = \frac{1}{2g(0)(4g(0) + 3)^2 \xi^2} \left[-8dg(0)\xi(g(0))^2 + 4(g(0))^2 \sqrt{9+12g(0)} \right. \\ \left. + 3dg(0)\xi \sqrt{9+12g(0)} + 16(g(0))^3 - 18dg(0)\xi g(0) \right. \\ \left. - 9\sqrt{9+12g(0)}g(0) + 48(g(0))^2 - 9dg(0)\xi + 27g(0) \right],$$

Finally the dynamics of the reduced system is determined by the equation

$$S' = AS + \mathbf{F}(S, \mathbf{h}(S)), \quad (\text{A.35})$$

which becomes

$$S' = -\frac{3}{2} \frac{4g(0) - \xi dg(0)}{\xi^2 g(0)(4g(0) + 3)} S^5 + \mathcal{O}(S^6). \quad (\text{A.36})$$

Hence for $g(0) > 0$, point E_6 is stable when $g(0) > \frac{\xi}{4} dg(0)$. Note how in this case the first non vanishing power in the S -expansion is S^5 , suggesting a highly non-linear dynamics for the center manifold.

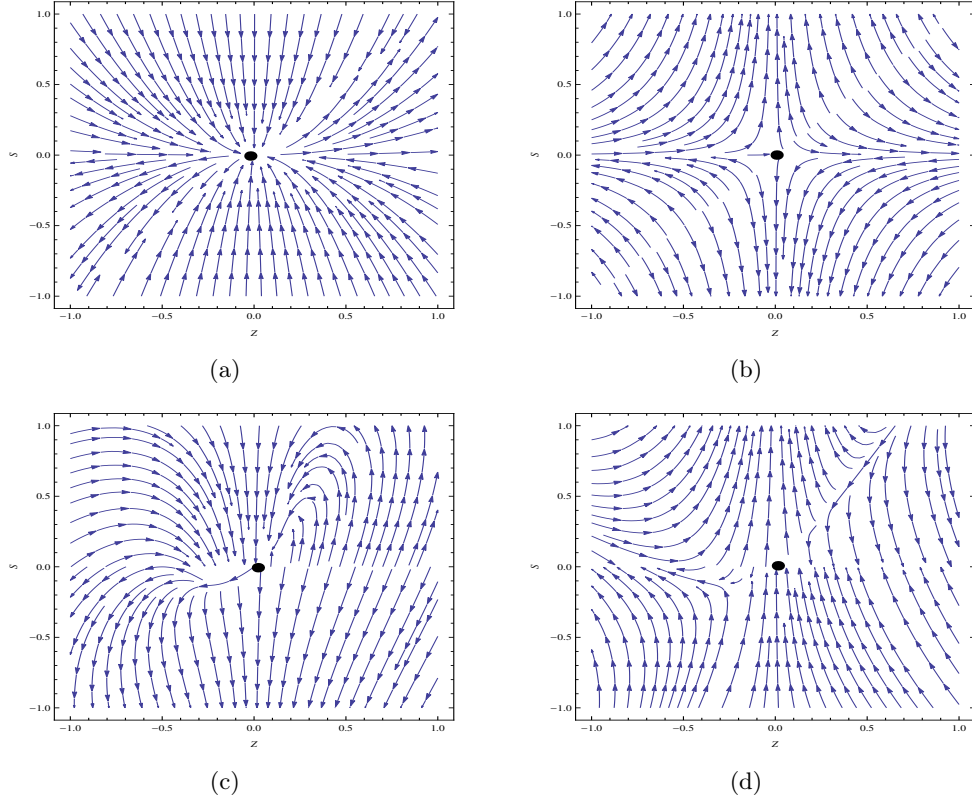


Figure 10: Phase portrait of the reduced system (A.41)-(A.42) in the $Z-S$ plane. In (a) we choose $\xi = -1$, $dg(0) = 0$, $d^2g(0) = -2$, in (b) $\xi = -1$, $dg(0) = 0$, $d^2g(0) = 2$, in (c) $\xi = -1$, $dg(0) = -1$, $d^2g(0) = 1$, in (d) $\xi = -1$, $dg(0) = 1$, $d^2g(0) = 1$.

Center manifold dynamics for point E_6 of model II when $g(0) = 0$

We finally explore the stability of point E_6 of model II (see Sec. 3.3.1) in the case where $g(0) = 0$. The first step (translation of point E_6 to the origin) is the same as the previous example. For the second step, using again the eigenvectors of the Jacobian matrix of the transformed system, we can introduce a new set of variables given by

$$\begin{pmatrix} X \\ Y \\ Z \\ S \end{pmatrix} = \begin{pmatrix} 1 & 0 & \frac{\xi}{\sqrt{6}} & \frac{1}{\sqrt{6}} \\ 0 & 1 & 0 & 0 \\ 0 & 0 & 1 & 0 \\ 0 & 0 & 0 & 1 \end{pmatrix} \begin{pmatrix} x \\ y \\ z \\ s \end{pmatrix}$$

In terms of these new set of variables, the system of equations can now be written as

$$\begin{pmatrix} X' \\ Y' \\ Z' \\ S' \end{pmatrix} = \begin{pmatrix} -3 & 0 & 0 & 0 \\ 0 & -3(1+w) & 0 & 0 \\ 0 & 0 & 0 & 0 \\ 0 & 0 & 0 & 0 \end{pmatrix} \begin{pmatrix} X \\ Y \\ Z \\ S \end{pmatrix} + \begin{pmatrix} g_1 \\ g_2 \\ f_1 \\ f_2 \end{pmatrix}$$

where f_1, f_2, g_1, g_2 are polynomials of degree greater than 2 in (X, Y, Z, S) with

$$\begin{aligned}
f_1(X, Y, Z, S) &= -3(w+1)ZY + \frac{3}{2}(1-w)ZX^2 - \frac{3}{2}(1+w)ZY^2 + \frac{\sqrt{6}}{2}w\xi Z^2X \\
&\quad + 3(1+w)Z^2Y - \frac{1}{4}(1+w)\xi^2Z^3 + \frac{\sqrt{6}}{2}(w-1)SZX - \frac{1}{2}w\xi SZ^2 \\
&\quad + \frac{1}{4}(1-w)S^2Z - \frac{3}{2}Z^2X^2(1-w) + \frac{3}{2}(w+1)Z^2Y^2 + \frac{\sqrt{6}}{2}\xi(1-w)Z^3X \\
&\quad - \frac{1}{4}(1-w)\xi^2Z^4 + \frac{\sqrt{6}}{2}(1-w)SZ^2X - \frac{1}{2}(1-w)\xi SZ^3 - \frac{1}{4}(1-w)S^2Z^2, \\
f_2(X, Y, Z, S) &= -\sqrt{6}g(S)X + g(S)\xi Z + g(S)S.
\end{aligned}$$

whereas g_1, g_2 are not shown due to their lengths. Now the coordinates over the 2D center manifold which correspond to the non-zero eigenvalues (X, Y) , can be approximated in terms of remaining coordinates Z, S by the functions (up to third order)

$$h_1(Z, S) = a_1Z^2 + a_2Z^3 + a_3ZS + a_4Z^2S + a_5S^2 + a_6ZS^2 + a_7S^3, \quad (\text{A.37})$$

$$h_2(Z, S) = b_1Z^2 + b_2Z^3 + b_3ZS + b_4Z^2S + b_5S^2 + b_6ZS^2 + b_7S^3, \quad (\text{A.38})$$

respectively. Then the quasilinear partial differential equation which the function vector

$$\mathbf{h} = \begin{pmatrix} h_1 \\ h_2 \end{pmatrix}$$

has to satisfy, is given by

$$D\mathbf{h}(\mathbf{U})[A\mathbf{U} + \mathbf{F}(\mathbf{U}, \mathbf{h}(\mathbf{U}))] - B\mathbf{h}(\mathbf{U}) - \mathbf{g}(\mathbf{U}, \mathbf{h}(\mathbf{U})) = \mathbf{0}, \quad (\text{A.39})$$

where

$$\mathbf{U} = (Z, S), \quad \mathbf{g} = \begin{pmatrix} g_1 \\ g_2 \end{pmatrix}, \quad \mathbf{F} = \begin{pmatrix} f_1 \\ f_2 \end{pmatrix}, \quad B = \begin{pmatrix} -3 & 0 \\ 0 & -3(1+w) \end{pmatrix}, \quad A = 0.$$

Equalling different powers of S and Z in Eq. (A.39) yields finally the values of the constants $a_1, a_2, a_3, a_4, a_5, a_6, a_7, b_1, b_2, b_3, b_4, b_5, b_6, b_7$ as:

$$\begin{aligned}
a_1 &= -\frac{\xi}{\sqrt{6}}, & a_2 &= -\frac{\xi}{\sqrt{6}}, & a_3 &= \frac{\sqrt{6}}{18}\xi dg(0), \\
a_4 &= \frac{\sqrt{6}}{18}\xi dg(0)\left(1 - \frac{dg(0)\xi}{3}\right) - \frac{\sqrt{6}}{36}\xi^2, & a_5 &= \frac{\sqrt{6}}{18}dg(0), \\
a_6 &= -\frac{\sqrt{6}\xi}{108(1+w)}\left(8dg(0)^2(w+1) - 3d^2g(0)(w+1) + 3(w-3)\right), \\
a_7 &= -\frac{\sqrt{6}}{36(w+1)}\left(2dg(0)^2(w+1) - d^2g(0)(w+1) - 4\right), \\
b_1 &= -\frac{\xi^2}{12}, & b_2 &= -\frac{\xi^2}{6}, & b_3 &= \frac{1}{6}\frac{\xi(1-w)}{1+w}, \\
b_4 &= \frac{\xi}{18(1+w)^2}\left(\xi dg(0)(w^2 + 2w - 1) + 3(1-w^2)\right), & b_5 &= \frac{3-w}{12(w+1)}, \\
b_6 &= \frac{\xi dg(0)(w^2 + w - 3)}{9(1+w)^2}, & b_7 &= \frac{dg(0)(w^2 - 5)}{18(1+w)^2}
\end{aligned} \quad (\text{A.40})$$

Finally the dynamics over the center manifold is determined by

$$Z' = -\frac{\xi}{2}Z^2S - \frac{1}{2}ZS^2, \quad (\text{A.41})$$

$$S' = dg(0)\xi ZS + dg(0)S^2 + dg(0)\xi S Z^2 + \left(\frac{1}{2}d^2g(0) - \frac{1}{3}dg(0)^2\right)\xi ZS^2 \\ + \left(\frac{1}{2}d^2g(0) - \frac{1}{3}dg(0)^2\right)S^3. \quad (\text{A.42})$$

where $d^2g(0)$ denotes the second order derivatives of g at $S = 0$. The full dynamics of the reduced 2D system (A.41)-(A.42) is complicated to determine analytically. We can however check its stability for few examples. In Fig. 10 we have plotted the phase portrait on the $Z - S$ plane choosing some values for the parameters ξ , $dg(0)$ and $d^2g(0)$. As one can see from the figure, the point E_6 is always saddle for these choices of parameters. Moreover, we have checked that for other choices of ξ , $dg(0)$ and $d^2g(0)$ point E_6 is still saddle. This suggests that point E_6 is a saddle for any combination of the parameters.

References

- [1] A. G. Riess *et al.* [Supernova Search Team Collaboration], *Astron. J.* **116**, 1009 (1998) [astro-ph/9805201].
- [2] S. Perlmutter *et al.* [Supernova Cosmology Project Collaboration], *Astrophys. J.* **517**, 565 (1999) [astro-ph/9812133].
- [3] M. Betoule *et al.* [SDSS Collaboration], *Astron. Astrophys.* **568** (2014) A22 [arXiv:1401.4064 [astro-ph.CO]].
- [4] P. A. R. Ade *et al.* [Planck Collaboration], *Astron. Astrophys.* **571**, A16 (2014) doi:10.1051/0004-6361/201321591 [arXiv:1303.5076 [astro-ph.CO]].
- [5] P. A. R. Ade *et al.* [Planck Collaboration], *Astron. Astrophys.* **594**, A13 (2016) doi:10.1051/0004-6361/201525830 [arXiv:1502.01589 [astro-ph.CO]].
- [6] L. Randall and R. Sundrum, *Phys. Rev. Lett.* **83**, 3370 (1999) doi:10.1103/PhysRevLett.83.3370 [hep-ph/9905221].
- [7] L. Randall and R. Sundrum, *Phys. Rev. Lett.* **83**, 4690 (1999) doi:10.1103/PhysRevLett.83.4690 [hep-th/9906064].
- [8] G. R. Dvali, G. Gabadadze and M. Porrati, *Phys. Lett. B* **485**, 208 (2000) doi:10.1016/S0370-2693(00)00669-9 [hep-th/0005016].
- [9] S. Weinberg, *Rev. Mod. Phys.* **61**, 1 (1989).
- [10] J. Martin, *Comptes Rendus Physique* **13**, 566 (2012) [arXiv:1205.3365 [astro-ph.CO]].
- [11] P. J. Steinhardt, L. M. Wang and I. Zlatev, *Phys. Rev. D* **59** (1999) 123504 doi:10.1103/PhysRevD.59.123504 [astro-ph/9812313].
- [12] E. J. Copeland, M. Sami and S. Tsujikawa, *Int. J. Mod. Phys. D* **15**, 1753 (2006) doi:10.1142/S021827180600942X [hep-th/0603057].
- [13] S. Tsujikawa, *Class. Quant. Grav.* **30**, 214003 (2013) doi:10.1088/0264-9381/30/21/214003 [arXiv:1304.1961 [gr-qc]].
- [14] C. M. Will, *Theory and experiment in Gravitational Physics*, Cambridge University Press, 1993.
- [15] C. M. Will, *Living Rev. Rel.* **17**, 4 (2014) doi:10.12942/lrr-2014-4 [arXiv:1403.7377 [gr-qc]].

- [16] Y. L. Bolotin, A. Kostenko, O. A. Lemets and D. A. Yerokhin, *Int. J. Mod. Phys. D* **24** (2014) no.03, 1530007 doi:10.1142/S0218271815300074 [arXiv:1310.0085 [astro-ph.CO]].
- [17] J. Väliiviita and E. Palmgren, *JCAP* **1507**, no. 07, 015 (2015) doi:10.1088/1475-7516/2015/07/015 [arXiv:1504.02464 [astro-ph.CO]].
- [18] B. Wang, E. Abdalla, F. Atrio-Barandela and D. Pavon, *Rept. Prog. Phys.* **79**, no. 9, 096901 (2016) doi:10.1088/0034-4885/79/9/096901 [arXiv:1603.08299 [astro-ph.CO]].
- [19] B. Gumjudpai, T. Naskar, M. Sami and S. Tsujikawa, *JCAP* **0506**, 007 (2005) doi:10.1088/1475-7516/2005/06/007 [hep-th/0502191].
- [20] G. Caldera-Cabral, R. Maartens and B. M. Schaefer, *JCAP* **0907**, 027 (2009) doi:10.1088/1475-7516/2009/07/027 [arXiv:0905.0492 [astro-ph.CO]].
- [21] C. Wetterich, *Astron. Astrophys.* **301**, 321 (1995) [hep-th/9408025].
- [22] L. Amendola, *Phys. Rev. D* **62**, 043511 (2000) doi:10.1103/PhysRevD.62.043511 [astro-ph/9908023].
- [23] W. Zimdahl and D. Pavon, *Phys. Lett. B* **521**, 133 (2001) doi:10.1016/S0370-2693(01)01174-1 [astro-ph/0105479].
- [24] S. M. Carroll, M. Hoffman and M. Trodden, *Phys. Rev. D* **68**, 023509 (2003) doi:10.1103/PhysRevD.68.023509 [astro-ph/0301273].
- [25] J. M. Cline, S. Jeon and G. D. Moore, *Phys. Rev. D* **70**, 043543 (2004) doi:10.1103/PhysRevD.70.043543 [hep-ph/0311312].
- [26] V. Salvatelli, N. Said, M. Bruni, A. Melchiorri and D. Wands, *Phys. Rev. Lett.* **113** (2014) no.18, 181301 doi:10.1103/PhysRevLett.113.181301 [arXiv:1406.7297 [astro-ph.CO]].
- [27] C. van de Bruck, J. Mifsud and J. Morrice, *Phys. Rev. D* **95** (2017) no.4, 043513 doi:10.1103/PhysRevD.95.043513 [arXiv:1609.09855 [astro-ph.CO]].
- [28] T. Yang, Z. K. Guo and R. G. Cai, *Phys. Rev. D* **91** (2015) no.12, 123533 doi:10.1103/PhysRevD.91.123533 [arXiv:1505.04443 [astro-ph.CO]].
- [29] C. Caprini and N. Tamanini, *JCAP* **1610** (2016) no.10, 006 doi:10.1088/1475-7516/2016/10/006 [arXiv:1607.08755 [astro-ph.CO]].
- [30] R. G. Cai, N. Tamanini and T. Yang, *JCAP* **1705** (2017) no.05, 031 doi:10.1088/1475-7516/2017/05/031 [arXiv:1703.07323 [astro-ph.CO]].
- [31] C. G. Boehmer, G. Caldera-Cabral, R. Lazkoz and R. Maartens, *Phys. Rev. D* **78**, 023505 (2008) doi:10.1103/PhysRevD.78.023505 [arXiv:0801.1565 [gr-qc]].
- [32] C. G. Boehmer, G. Caldera-Cabral, N. Chan, R. Lazkoz and R. Maartens, *Phys. Rev. D* **81**, 083003 (2010) doi:10.1103/PhysRevD.81.083003 [arXiv:0911.3089 [gr-qc]].
- [33] J. Dutta, W. Khylllep and E. Syiemlieh, *Eur. Phys. J. Plus* **131**, no. 2, 33 (2016) doi:10.1140/epjp/i2016-16033-7 [arXiv:1602.03329 [gr-qc]].
- [34] J. Valiviita, E. Majerotto and R. Maartens, *JCAP* **0807** (2008) 020 doi:10.1088/1475-7516/2008/07/020 [arXiv:0804.0232 [astro-ph]].
- [35] V. Faraoni, J. B. Dent and E. N. Saridakis, *Phys. Rev. D* **90** (2014) no.6, 063510 doi:10.1103/PhysRevD.90.063510 [arXiv:1405.7288 [gr-qc]].
- [36] C. Skordis, A. Pourtsidou and E. J. Copeland, *Phys. Rev. D* **91** (2015) no.8, 083537 doi:10.1103/PhysRevD.91.083537 [arXiv:1502.07297 [astro-ph.CO]].
- [37] N. Tamanini, *Phys. Rev. D* **92**, no. 4, 043524 (2015) doi:10.1103/PhysRevD.92.043524 [arXiv:1504.07397 [gr-qc]].

- [38] C. G. Boehmer, N. Tamanini and M. Wright, Phys. Rev. D **91**, no. 12, 123002 (2015) doi:10.1103/PhysRevD.91.123002 [arXiv:1501.06540 [gr-qc]].
- [39] C. G. Boehmer, N. Tamanini and M. Wright, Phys. Rev. D **91**, no. 12, 123003 (2015) doi:10.1103/PhysRevD.91.123003 [arXiv:1502.04030 [gr-qc]].
- [40] J. D. Brown, Class. Quant. Grav. **10** (1993) 1579 [gr-qc/9304026].
- [41] T. S. Koivisto, E. N. Saridakis and N. Tamanini, JCAP **1509** (2015) 047 doi:10.1088/1475-7516/2015/09/047 [arXiv:1505.07556 [astro-ph.CO]].
- [42] C. G. Boehmer, N. Tamanini and M. Wright, Phys. Rev. D **92**, no. 12, 124067 (2015) doi:10.1103/PhysRevD.92.124067 [arXiv:1510.01477 [gr-qc]].
- [43] P. Brax and N. Tamanini, Phys. Rev. D **93** (2016) no.10, 103502 doi:10.1103/PhysRevD.93.103502 [arXiv:1512.07399 [astro-ph.CO]].
- [44] N. Tamanini and M. Wright, JCAP **1604** (2016) no.04, 032 doi:10.1088/1475-7516/2016/04/032 [arXiv:1602.06903 [gr-qc]].
- [45] J. Dutta, W. Khyllep and N. Tamanini, Phys. Rev. D **95**, no. 2, 023515 (2017) (arXiv:1701.00744 [gr-qc]).
- [46] W. Fang, Y. Li, K. Zhang and H. Q. Lu, Class. Quant. Grav. **26** (2009) 155005 doi:10.1088/0264-9381/26/15/155005 [arXiv:0810.4193 [hep-th]].
- [47] J. Dutta, W. Khyllep and N. Tamanini, Phys. Rev. D **93**, no. 6, 063004 (2016) doi:10.1103/PhysRevD.93.063004 [arXiv:1602.06113 [gr-qc]].
- [48] Y. Leyva, D. Gonzalez, T. Gonzalez, T. Matos and I. Quiros, Phys. Rev. D **80**, 044026 (2009) doi:10.1103/PhysRevD.80.044026 [arXiv:0909.0281 [gr-qc]].
- [49] D. Escobar, C. R. Fadrugas, G. Leon and Y. Leyva, Class. Quant. Grav. **29**, 175005 (2012) doi:10.1088/0264-9381/29/17/175005 [arXiv:1110.1736 [gr-qc]].
- [50] D. Escobar, C. R. Fadrugas, G. Leon and Y. Leyva, Class. Quant. Grav. **29**, 175006 (2012) doi:10.1088/0264-9381/29/17/175006 [arXiv:1201.5672 [gr-qc]].
- [51] I. Quiros, T. Gonzalez, D. Gonzalez and Y. Napoles, Class. Quant. Grav. **27**, 215021 (2010) doi:10.1088/0264-9381/27/21/215021 [arXiv:0906.2617 [gr-qc]].
- [52] W. Fang and H. Q. Lu, Eur. Phys. J. C **68**, 567 (2010) doi:10.1140/epjc/s10052-010-1352-0 [arXiv:1007.2330 [hep-th]].
- [53] H. Farajollahi, A. Salehi, F. Tayebi and A. Ravanpak, JCAP **1105**, 017 (2011) doi:10.1088/1475-7516/2011/05/017 [arXiv:1105.4045 [gr-qc]].
- [54] G. Leon, Y. Leyva and J. Socorro, Phys. Lett. B **732**, 285 (2014) doi:10.1016/j.physletb.2014.03.053 [arXiv:1208.0061].
- [55] K. Xiao and J. Y. Zhu, Phys. Rev. D **83**, 083501 (2011) doi:10.1103/PhysRevD.83.083501 [arXiv:1102.2695 [gr-qc]].
- [56] S. Wiggins, *Introduction to Applied Nonlinear Dynamical Systems and Chaos*. (Springer, New York Heidelberg Berlin, 1990).
- [57] L. Perko, *Differential Equations and Dynamical Systems*. (SpringerVerlag, 1991).
- [58] N. Tamanini, *Dynamical systems in DE models*, PhD thesis, University College London (2014).
- [59] C. G. Boehmer, N. Chan and R. Lazkoz, Phys. Lett. B **714** (2012) 11 doi:10.1016/j.physletb.2012.06.064 [arXiv:1111.6247 [gr-qc]].
- [60] N. Tamanini, Phys. Rev. D **89** (2014) 083521 doi:10.1103/PhysRevD.89.083521 [arXiv:1401.6339 [gr-qc]].

- [61] Y. F. Cai, E. N. Saridakis, M. R. Setare and J. Q. Xia, Phys. Rept. **493** (2010) 1
doi:10.1016/j.physrep.2010.04.001 [arXiv:0909.2776 [hep-th]].